Matrix Biology 131 (2024) 62–76

Contents lists available at ScienceDirect

Matrix Biology

journal homepage: www.elsevier.com/locate/matbio

Ameloblastin and its multifunctionality in amelogenesis: A review

Natalie C. Kegulian [1], Gayathri Visakan [1], Rucha Arun Bapat, Janet Moradian-Oldak [*]

Center for Craniofacial Molecular Biology, Herman Ostrow School of Dentistry, University of Southern California, 2250 Alcazar St., CSA 148, Los Angeles, CA 90033, USA

ARTICLE INFO

Keywords:
Enamel
Amelogenesis
Ameloblastin
Protein multifunctionality
Matricellular proteins
Ameloblasts
Amphipathic helix

ABSTRACT

Extracellular matrix proteins play crucial roles in the formation of mineralized tissues like bone and teeth via multifunctional mechanisms. In tooth enamel, ameloblastin (Ambn) is one such multifunctional extracellular matrix protein implicated in cell signaling and polarity, cell adhesion to the developing enamel matrix, and stabilization of prismatic enamel morphology. To provide a perspective for Ambn structure and function, we begin this review by describing dental enamel and enamel formation (amelogenesis) followed by a description of enamel extracellular matrix. We then summarize the established domains and motifs in Ambn protein, human *amelogenesis imperfecta* cases, and genetically engineered mouse models involving mutated or null *Ambn*. We subsequently delineate *in silico, in vitro*, and *in vivo* evidence for the amphipathic helix in Ambn as a proposed cell-matrix adhesive and then more recent *in vitro* evidence for the multitargeting domain as the basis for dynamic interactions of Ambn with itself, amelogenin, and membranes. The multitargeting domain facilitates tuning between Ambn-membrane interactions and self/co-assembly and supports a likely overall role for Ambn as a matricellular protein. We anticipate that this review will enhance the understanding of multifunctional matrix proteins by consolidating diverse mechanisms through which Ambn contributes to enamel extracellular matrix mineralization.

Tooth enamel and amelogenesis

Tooth enamel is formed by ameloblast cells through a process called amelogenesis. It is the hardest tissue in the mammalian body, comprising approximately 95 % mineral [1,2]. Mature enamel is composed of calcium hydroxyapatite (HAP) crystals with small amounts of fluoride, carbonate, and magnesium [3]. The earliest formed mineral in enamel is amorphous calcium phosphate (ACP) [4], which later transforms into apatite crystallites with a magnesium- and carbonate-enriched core [5]. In humans, pigs, mice, and rats, among other mammals, enamel crystals are organized into a prismatic structure, in which HAP crystals are packed into rods (also known as prisms). The rods are the basic structural units of enamel, running from the dentino-enamel junction (DEJ) to the surface of the enamel [6]. In prismatic enamel, rods are interspersed with interrod enamel, which also is made up of HAP crystals that are oriented at different angles to the rods [7–9]. They form a decussating pattern [5], which is the result of movements of ameloblast cells in different directions [10]. One rod originates from one ameloblast, while interrod enamel is formed via synchronized secretion by several neighboring ameloblasts within a row [11–14]. The overall direction of each prism represents the fossilized path traced out during amelogenesis by the Tomes' process [15–17], which is a protuberance that projects from each ameloblast into the extracellular matrix (ECM) at the early stage of amelogenesis [18].

Abbreviations: ACP, amorphous calcium phosphate; AFM, atomic force microscopy; AH, amphipathic helix; *AI*, *amelogenesis imperfecta*; Ambn, ameloblastin; AmbnΔ5, Ambn with deletion of the sequence encoded by exon 5; AmbnΔ6, Ambn with deletion of the sequence encoded by exon 6; Amel, amelogenin; Amtn, amelotin; CD, circular dichroism; co-IP, co-immunoprecipitation; DEJ, dentino-enamel junction; DLS, dynamic light scattering; ECM, extracellular matrix; EMP, enamel matrix protein; Enam, enamelin; EPR, electron paramagnetic resonance; FRET, fluorescence resonance energy transfer; HAP, hydroxyapatite; KLK-4, kallikrein-related peptidase-4; LAMP1, lysosome-associated membrane protein-1; LUV, large unilamellar vesicle; MMP-20, matrix metalloproteinase-20; NMR, nuclear magnetic resonance; Odam, odontogenic ameloblast-associated; SCPP, secretory calcium-binding phosphoprotein; Scpppq1, secretory calcium-binding phosphoprotein proline-glutamine rich 1; SDSL, site-directed spin-labeling; TEM, transmission electron microscopy; TRAP, tyrosine-rich Amel peptide; Y2H, yeast two-hybrid.

* Corresponding author.
E-mail address: joldak@usc.edu (J. Moradian-Oldak).
[1] Equal Contribution.

https://doi.org/10.1016/j.matbio.2024.05.007
Received 2 April 2024; Received in revised form 16 May 2024; Accepted 24 May 2024
Available online 28 May 2024

Unlike mammals, non-mammalian tetrapods have aprismatic enamel, comprising parallel bundles of HAP crystallites that are arranged perpendicular to the tooth surface [15,19]. The prismatic enamel architecture of mammalian vertebrates has been attributed to the evolution of Tomes' processes projecting from the ameloblasts of these animals, in contrast to the absence of Tomes' processes from ameloblasts of non-mammalian vertebrates [8,20]. Analogously, the formation of an outermost layer of enamel that is devoid of prismatic crystal arrangement in most mammalian species has been attributed to the loss of the Tomes' processes during the transition stage of amelogenesis [15,21]. However, others contend that the assumptions about correlations in the shape of the cells at the mineralizing front and the type of enamel prisms cannot be extended to explain the formation of aprismatic enamel. While the shape of the cells is an important factor, it may not alone explain the full range of observed structures in non-mammalian vertebrates [22].

Amelogenesis involves two main stages, secretory and maturation, which are linked by a transition stage between the two [9] and preceded by a presecretory stage [23]. Progression through the stages is directed by several types of epithelial cells organized in layers of the enamel organ [2] and by epithelium-mesenchyme interactions [24]. During the onset of presecretory stage, the innermost layer of epithelial cells within the enamel organ, called the inner enamel epithelium, differentiates into ameloblasts [2]. Ameloblasts secrete structural enamel matrix proteins (EMPs), proteases, and inorganic components that then interact in the ECM space to form enamel [25]. The process involves a sequence of steps encompassing both major stages that are regulated by a number of genes and signaling pathways [26].

During secretory stage, ameloblasts are differentiated into highly polarized, columnar cells with Tomes' processes [7]. Tomes' processes are picket fence-like cytoplasmic extensions of secretory ameloblasts that are present in mammalian tetrapods [20,27,28]. In maturation stage, ameloblasts are wider and shorter than secretory ameloblasts, have no Tomes' processes, and alternate between smooth and ruffled edges at the enamel surface [1]. Maturation-stage ameloblasts secrete a different ensemble of proteins from those produced by secretory-stage ameloblasts. They cycle between ruffled and smooth-edged cell morphologies, secrete ions for building more enamel mineral crystals and regulating pH, endocytose debris from EMPs previously released into the ECM, and ultimately undergo apoptosis when enamel production is complete [2].

Amelogenin and other EMPs

The main EMPs secreted by ameloblasts into the ECM during secretory stage are the structural proteins amelogenin (Amel), ameloblastin (Ambn), enamelin (Enam), and the protease matrix metalloproteinase-20 (MMP-20), also known as enamelysin [7]. Mutations in each of these EMPs have been associated with cases in humans of *amelogenesis imperfecta* (*AI*), an umbrella term for different syndromes characterized by hypoplastic or hypomineralized enamel [29] (for more about *AI*, see section "Ambn in *AI*"). Amel is the major component of the developing enamel matrix [25]. Genes for Ambn, Enam, and other members of the secretory calcium-binding phosphoprotein (SCPP) family evolved from a common ancestral gene in vertebrates [30]. Among SCPP genes, only *AMEL* is located not on chromosome 4 but on chromosomes X and Y [25,31]. Through extensive *in vitro* and *in vivo* studies, the roles of Amel have been identified as control of enamel thickness, control of ACP-to-HAP mineral phase transformation, and the elongation and organization of HAP crystals into rods [25,32–35]. Among other mechanisms, crystal elongation and organization were proposed to occur through the templating of mineral via Amel self-assembly in parallel to the crystal growth [36,37] and cooperation between Amel and other EMPs [38]. Amel is phosphorylated at serine-16 [25], a modification critical for Amel-mediated stabilization of the ACP phase, HAP crystal orientation within the rods, and compositional characteristics of dental enamel [39–41].

Amel is a proline-rich intrinsically disordered protein containing a large, highly hydrophobic core [42] flanked by a hydrophobic functional domain and a hydrophilic C-terminal end [43]. The N- and C-termini of Amel are evolutionarily conserved among species, indicating their critical roles in amelogenesis [44]. Snead et al. defined domain "A" (the first 42 aa at the N-terminal end) as implicated in Amel self-assembly interactions [43]. Expression of a transgenic Amel lacking domain "A" in mouse resulted in abnormal enamel matrix patterning due to defective Amel nanosphere formation, which was reflected in the dysmorphic architecture of enamel rods in this mouse [45]. Subsequent to this model, an evolutionarily conserved motif with a general sequence of Y/F-x-x-Y/L/F-x-Y/F was identified and revealed to be shared by Amel and Ambn across tetrapod species and essential for self-assembly by both proteins [46]. Amel domain "A" contains two incidences in its sequence of the Y/F-x-x-Y/L/F-x-Y/F, amino acids 12–17 and 33–38 in the human sequence, via which it self-assembles [46]. The motif from residues 33 to 38 is also part of a lectin-binding motif [47], disruptions in which are associated with hypomineralization/hypomaturation *AI* [48].

While maturation-stage ameloblasts' expression of MMP-20 is greatly reduced, they secrete another major protease in this stage, kallikrein-related peptidase-4 (KLK-4) [7], as well as different structural EMPs from those that dominate secretory stage, chiefly amelotin (Amtn) [49,50], odontogenic ameloblast-associated (Odam), and secretory calcium-binding phosphoprotein proline-glutamine rich 1 (Scpppq1) [51]. EMPs diverged earlier in evolution than the emergence of enamel, contain computationally identified motifs that have not been linked to their enamel functions, and are associated with non-oral phenotypes in animal models, all of which substantiates pleiotropy of their functions and repurposing of their genes from older functions towards supporting amelogenesis [52–54]. Notwithstanding, this review will focus mainly on Ambn functions in enamel and the growing body of knowledge of its interactions with cells and with Amel. While Amel structure and function have been extensively covered in past reviews [55–57], no review prior to this one has focused on Ambn and comprehensively summarized *in vitro* and *in vivo* findings on its structure and functions. The emerging multifunctionality of Ambn places it among other multifunctional proteins of the mineralizing matrix in bones and teeth such as bone sialoprotein, osteopontin, osteocalcin, dentin sialophosphoprotein, and dentin matrix protein 1, which, while originally regarded exclusively as crystal nucleators and destroyers, are now known to participate in cell adhesion, inflammation, nervous system activity, aging, apoptosis, and other processes [58–64].

Ambn: *AI* cases, animal models, and classical functions and motifs

Ambn was first observed in porcine enamel ECM in the early 1990s by Uchida et al. [65,66], initially as non-Amel protein fragments ranging from 13 to 17 kDa in the sheath space between rod and interrod enamel and then as 40- and 62 kDa parent proteins. Hu et al [67] subsequently matched these non-amelogenins to cDNA sequences in a porcine enamel organ epithelia-specific cDNA library and identified two proteins about 40 and 42 kDa in mass. It was then determined that they were alternatively spliced variants and the 13–17 kDa protein fragments were their enzymatic cleavage products. They called the entire group of these proteins sheathlin because of the location of the cleavage products. Concomitantly, Cerny et al. [68] found mRNA expressed in rat ameloblasts encoding 407- and 324-amino acid proteins that they named amelin 1 and amelin 2.

Ambn is the second most abundant EMP after Amel, and like Amel it is proline- and glutamine-rich and intrinsically disordered [46,69–71]. Within the N-terminal region, Ambn is phosphorylated at a serine residue and O-glycosylated within a 15-amino-acid stretch that is present in one of its two alternatively spliced variants [72]. In its C-terminal

region, Ambn has at least one sulfated O-glycosylation as well [73]. Along with Amel, Ambn is secreted by ameloblasts and rapidly processed at its C-terminal end [74]. Proteolytic cleavage of Amel, Ambn, and Enam by MMP-20 during secretory stage produces a variety of cleavage products of each EMP that more effectively aid in enamel rod formation by assuming different roles in the ECM [74,75]. In contrast, cleavage by KLK-4 during maturation stage degrades EMPs and their fragments completely to eliminate almost all organic matter from the final enamel product [25], resulting in the characteristic hardness of dental enamel [76].

Following a genome project aimed at discovering novel tooth development genes [77], Krebsbach et al. fully sequenced the *Ambn* gene, whose similarity to Cerny et al.'s amelin 1 and amelin 2 mRNA sequences indicated that they were transcribed from the same gene [69]. It became clear from high sequence similarity and the respective locations of parent and fragment protein products that the sheathlin found in porcine enamel and the amelin found in the ECM secreted by rat ameloblasts are the same protein, which came to be mainly called ameloblastin (reviewed in [78]). The human *AMBN* gene was then mapped to human chromosome 4q21 [79], a region to which the locus for autosomal dominant local hypoplastic *AI* had been mapped. That form of *AI* was subsequently linked to a nonsense mutation in the gene encoding Enam [80], which is also on 4q21.

Ambn in AI

In human, mutations in *AMBN* have been associated with *amelogenesis imperfecta* (*AI*) [29]. In *AI* patients with mutations in *AMBN*, enamel phenotypes vary widely. Enamel appeared hypoplastic (i.e., thin) or at times aprismatic, and, in some cases, the underlying dentin was also affected [81–84]. In addition, a polymorphism in *AMBN* was associated with molar hypomineralization when present in conjunction with taking medications before 4 years of age [85]. The nine known cases, or groups of cases, of *AI* associated with *AMBN* gene defects are enumerated in Table 1. The first such reported case was a deletion of *AMBN* exon 6 in a second cousin consanguineous Costa Rican family [81]. Three of the six children had rough hypoplastic *AI*, with a thin layer of poorly formed enamel mineral in some regions and none in others, as observed by high-resolution x-ray CT scanning. A fourth child was heterozygous for the mutation and only had very minor enamel defects.

Another case of *AMBN*-related *AI* was a patient referred to a study piloting a targeted next-generation sequencing assay for pinpointing novel mutations associated with orodental disease [84]. This patient, like those in the previous study with the exon 6 deletion, had a limited layer of hypoplastic enamel. The mutation was found to be a substitution at a splice site of *AMBN*, causing either retention of intron 6 or exclusion of exon 7. The former was predicted to lead to nonsense-mediated decay of the resulting protein, while the latter could produce either the same response or an internally truncated Ambn protein. The patient was homozygous for the mutation and thus had no normal Ambn.

A substitution mutation in exon 13 of *AMBN* was found in a Chinese family with a considerably different *AI* phenotype, as the underlying dentin in these patients was also affected [82]. The patients were heterozygous for the mutation and had thin, chipping enamel and loose teeth. Scanning electron microscopy (SEM) revealed that, contrary to previously discovered *AMBN*-associated *AI* cases, enamel still had some prismatic structure, albeit with areas of structural disturbance and fewer prisms overall. Furthermore, abnormalities in dentin were observed, namely uneven dentin tubule distribution with abnormally small dentin tubules and thickened peritubular dentin. This was the first example of *AI* associated with an *AMBN* mutation affecting dentin structure.

The fourth example of *AMBN* mutation-associated *AI* was found in a Hispanic family in which the proband was the only member with severe *AI* [83]. This individual had compound heterozygosity for two missense mutations in *AMBN*, one copy of the gene having a substitution mutation changing leucine-354 to proline and the other with a mutation changing proline-447 to leucine. Both were bioinformatically revealed to be highly conserved residues. The patient's teeth had thin or no enamel and were severely worn down. Heterozygotes for the mutation at residue 354 had only mild pitting of dental surfaces, and no recruited members had the mutation at residue 447 in isolation.

Finally, several families showing *AI* phenotypes associated with five *AMBN* mutant genotypes were identified in a recent study [86]. The following genotypes were all clinically similar, namely resulting in a similar phenotype: 1. Homozygotes for a nonsense mutation changing serine-70 to a stop codon. 2. Compound heterozygotes for this same mutation on one *AMBN* copy and a missense mutation changing tyrosine-99 to histidine on the other. 3. Compound heterozygotes with a frameshift-causing duplication where valine-81 is encoded that is predicted to result in nonsense-mediated decay in one allele and a mutation that alters a splice site and results in exon skipping in the other. *AI* patients within these families had thin, poor-quality enamel, and their teeth were yellow in appearance due to early post-eruption loss of soft, hypomineralized tissue. Other patients in the study, comprising a second clinical group unrelated to the severely affected homozygotes in the first group, were heterozygous for the same nonsense mutation at the site encoding serine-70. Their phenotype was less severe and involved hypomaturation *AI* with pitting and a near-normal enamel volume.

Table 1
Reported cases of *AI* in which an *AMBN* mutation was implicated.

Genotype	Inheritance pattern	Phenotype	Reference (s)
AMBN exon 6 deletion	Autosomal recessive	Rough-surfaced, pitted teeth, hypoplastic enamel lacking prismatic structure except in very few regions of poorly formed prisms, some regions with no enamel	[81]
c532-1G>C mutation at intron 6/exon 7 splice site, predicted to result in inclusion of the intron or exclusion of the exon	Autosomal recessive	Yellowed molars with a thin, hypoplastic enamel layer	[84]
c.1069C>T/ p. $Pro^{357}Ser$ mutation in exon 13	Autosomal dominant	Chipped, loose teeth, hypoplastic enamel with reduced number of prisms, and defective dentin with small, frequently occluded tubules	[82]
c.1061T>C/ p. $Leu^{354}Pro$ and c. 1340C>T/ p. $Pro^{447}Leu$	Autosomal recessive (compound heterozygosity)	Thin, almost nonexistent layer of enamel with dental attrition and hypoplasia	[83]
c.209C>G/ p.$Ser^{70}X$ nonsense mutation	Autosomal recessive	Hypoplastic enamel with early posteruption loss of mineralized tissue and subsequently yellow teeth	[86]
c.539dup/ p. $Val^{181}SerfsX5$ and c.571G>C/ p.?	Autosomal recessive (compound heterozygosity)		
c.209C>G/ p.$Ser^{70}X$ and c.295T>C/ p. $Tyr^{99}His$	Autosomal recessive (compound heterozygosity)		
c.209C>G/ p.$Ser^{70}X$	Autosomal dominant	Hypomature enamel with pitting and near-normal enamel volume	[86]
c.76G>A p.$Ala^{26}Thr$	Autosomal dominant	White, hypoplastic enamel that remains after tooth eruption	[86]

Heterozygotes for a missense mutation changing alanine-26 to threonine, forming a third clinical group, had hypoplastic *AI* with more persistent enamel and therefore whiter teeth than those of the first clinical group.

While most *AMBN*-associated *AI* cases involve hypoplastic enamel (all thus far except c.209C>G/ p.Ser^{70}X heterozygotes), their phenotypes vary noticeably in appearance and clinical presentation. This considerable heterogeneity, even among cases with the same mutation in one instance, could point to Ambn being a multifunctional protein and having several interaction partners.

Animal models

The *AI* cases caused by *AMBN* mutations described above demonstrate the complexity of enamel formation and are a clear indication that Ambn is critical for normal enamel formation. The mutations on *AMBN* gene produce Ambn protein with defective structure and function leading to enamel malformation and phenotypes that can be clinically identified. However, unraveling molecular and cellular mechanisms that govern the role of Ambn in amelogenesis cannot be explored in human cases of *AI*. Application of genetically engineered mice partially allowed exploration of Ambn roles at the cellular and molecular levels.

To date, over nineteen strains of *Ambn* knockout, transgenic, and mutant mouse models have been reported, and they support the notion that Ambn is critical for proper enamel formation (Table 2). Overexpression of *Ambn* in two transgenic models created against an Amelx-null (*Amelx*$^{-/-}$) background interfered in enamel rod architecture [87, 88] and resulted in dramatically shortened enamel crystals [88]. Other *Ambn* transgenic mouse models showed a correlation between the amount of expressed Ambn protein and their enamel mineral content, indicating a direct role of Ambn in the process of HAP crystal formation [89]. Severe enamel defects in an *Ambn* transgenic mouse in which serine residues were replaced by alanine supported the critical function of serine phosphorylation in Ambn [90]. The teeth of *Ambn* mutant mice lacking exons 5 and 6 (*Ambn*$^{\Delta 5\text{-}6}$) had a severely hypoplastic mineral layer atop the dentin layer, accompanied by dental and junctional epithelium defects, detachment of ameloblasts from the mineralizing ECM, and a decrease in *Amelx* gene expression [91,92]. The severe epithelial defects brought to light that *Ambn* mutations affect not only the structure of the enamel itself but also the integrity of the ameloblasts and their cell-matrix interactions. Ameloblast detachment from the ECM was also observed in *Ambn* overexpression models (Table 2). However, the detachment occurred in maturation stage and was associated with retention of EMPs in ameloblast cells and their matrix and abnormal deposits of EMPs at the points of detachment [93]. This recent set of transgenic models overexpressing *Ambn* showed localized enamel opacities due to hypomineralization, delayed ameloblast maturation stage, retention of Ambn and Amel in cysts in the enamel organ, and reduced endocytosis [93].

The enamel of *Ambn* knockout/*NLS-lacZ* knockin mice was hypoplastic and exhibited a very similar ameloblast pathology to those of the *Ambn*$^{\Delta 5\text{-}6}$ mutant mice, except that these animals also showed mineralized deposits of Amel protein on the dentin layer, indicating that *Amelx* expression was not reduced [83]. In *Ambn*$^{G/G}$ mutant mice, which were generated by targeted mutation to eliminate the Ambn self-assembly motif, enamel was hypomineralized with a disorganized structure, while *Ambn*$^{-/-}$ mice had only a residual layer of mineral atop their dentin [46]. To study amelogenesis via stage-specific labeling and gene alterations, a toolkit of mouse models was recently developed with modifications made to enamel-specific genes, including five made to *Ambn: Ambn-Cre, Ambn-IRESCre* (see Table Footnotes) *, Ambn-CreERT2, Ambn-p2A-eGFP,* and *Ambn-fl* [94]. These mice can be crossed with a variety of strains to knockout specific genes in or labeling of *Ambn* expressing cells, or to knock out *Ambn* itself in a timed manner, facilitating high-resolution studies of amelogenesis-related gene expression and cell signaling events.

Table 2
Mouse models of the major *Ambn* knock-out, deletion, mutation, or modulated-expression studies.

Model or group of models	Description	Phenotype	Reference(s)
Overexpressed *Ambn*	*Ambn* transgene regulated by the *Amelx* promoter	Crystallite abnormalities, increase in interrod enamel, decrease in rod enamel	[87]
Overexpressed *Ambn* against an *Amelx*$^{-/-}$ background	Crossed transgenic *Ambn*-overexpressing mice with *Amelx*$^{-/-}$ mice	Short, randomly oriented crystals, resembling the thin enamel layer on iguana teeth	[88]
Underexpressed, normally expressed, and overexpressed *Ambn* against an *Ambn*$^{-/-}$ background	Crossed *Ambn*$^{-/-}$ mice with *Ambn* transgenic mice expressing the transgene at low (*Ambn*$^{-/-, Tg+}$), normal (*Ambn*$^{-/-, Tg++}$), and high concentrations (*Ambn*$^{-/-, Tg+++}$)	*Ambn*$^{-/-, Tg++}$ mice had the closest amounts of enamel volume, mineral weight, and mineral density to WT mice. Both *Ambn*$^{-/-, Tg+}$ and *Ambn*$^{-/-, Tg+++}$ mice had reduced amounts compared to WT	[89]
Ambn overexpressed to different extents	Crossed transgenic *Ambn*-overexpressing mice with wild-type mice, which generated four concentrations of overexpressed *Ambn* (*Ambn*$^{Tg+}$, *Ambn*$^{Tg++}$, *Ambn*$^{Tg+++}$, and *Ambn*$^{Tg+++/++++}$)	Defects on all transgenic mice were Ambn dose-dependent (increasing from *Ambn*$^{Tg+}$ to *Ambn*$^{Tg+++/++++}$) and included localized incisor enamel lesions, delayed onset of maturation, cell-matrix detachment, retention of cell polarity, Ambn- and Amel-containing deposits and cysts in the enamel organ, and decreased endocytotic function	[93]
Overexpressed *Ambn* with residues Ser^{48}, Ser^{226}, and Ser^{2267} mutated to Ala (block phosphorylation) or to Asp (mimic phosphorylation)	*Ambn* transgene with triple Ser-Ala (*Ambn*$^{Tg\text{-}A}$) or Ser-Asp (*Ambn*$^{Tg\text{-}D}$) mutation expressed at higher-than-normal (*Ambn*$^{Tg\text{-}A+}$ or *Ambn*$^{Tg\text{-}D+}$) and much-higher-than-normal (*Ambn*$^{Tg\text{-}A++}$ or *Ambn*$^{Tg\text{-}D++}$) levels	Extensive, dose-dependent enamel defects including disorganized rod-interrod architecture and amorphous intervening layers in *Ambn*$^{Tg\text{-}A+}$ and *Ambn*$^{Tg\text{-}A++}$ mice, significantly less severe defects in enamel of *Ambn*$^{Tg\text{-}D+}$ and *Ambn*$^{Tg\text{-}D++}$ mice	[90]
Ambn lacking exons 5 and 6 (*Ambn*$^{\Delta 5\text{-}6}$)	*Ambn* gene was disrupted by homologous recombination, deleting exons 5 and 6, yielding	Detachment of ameloblasts from matrix and loss of cell polarity in secretory phase, irregular	[91,92]

(*continued on next page*)

Table 2 (*continued*)

Model or group of models	Description	Phenotype	Reference(s)
	an internally truncated protein ($Ambn^{\Delta 5\text{-}6}$) lacking the two exons	mineralized masses deposited on dentin instead of true enamel	
Ambn knockout/ *NLS-lacZ* knockin ($Ambn^{lacZ/lacZ}$ or $Ambn^{-/-}$)	Replaced a 4,204-bp piece of the *Ambn* gene with a gene encoding β-galactosidase, resulting in no *Ambn* expression	Rough-surfaced, hypomineralized teeth, ameloblasts detached from the mineralizing matrix, Amel protein-rich mineral nodules deposited on the dentin with a complete absence of enamel ribbons	[83]
Ambn lacking the Y/F-x-x-Y/L/F-x-Y/F self-assembly motif	Mutated the Y^{41}, Leu^{44}, and Phe^{46} to G to yield the triply mutated $Ambn^{G/G}$	Hypomineralized enamel with simple radial organization and expansion of the interrod region with no decussating rod pattern	[46]
Ambn-null	Frameshift mutation in exon 5 of the *Ambn* sequence resulting in no expression ($Ambn^{-/-}$)	Residual layer of thin, amorphous, enamel-like mineral crust	[46]
Ambn-Cre; Ambn-IRESCre	5' portion of one *Ambn* allele replaced with *Cre; Cre* inserted after *Ambn* stop codon using internal ribosomal entry site (IRES)	Like wild-type when heterozygous	[94]-Enamelbase[a]
Ambn-CreERT2	5' portion of one *Ambn* allele replaced with *CreERT2*	Like wild-type when heterozygous	[94]
Ambn-p2A-eGFP	Reporter allele made by fusing 3' end of *Ambn* to *eGFP* via *p2A* linker	Like wild-type with incisors showing a green fluorescent ameloblast layer	[94]
Ambn-fl	Flox allele made by inserting LoxP sites before and after exon 2	Like wild-type when crossed with mice expressing *Cre* in ameloblasts, shows severely impaired enamel mineralization similar to *Ambn*-null.	[94]

[a] https://www.facebase.org/resources/enamelbase/mouse-models/.

Altogether, *Ambn*-altered mouse models have demonstrated that Ambn is important for formation of enamel prismatic structure and for ameloblast cell integrity and function. In particular, elimination of the Y/F-x-x-Y/L/F-x-Y/F motif showed Ambn self-assembly to play a role in the organization of prisms, and deletion of exons 5 and 6 showed that the region they encode is important for enamel formation and ameloblast function. Overexpression and underexpression models showed that both having too much and having too little Ambn are detrimental to amelogenesis. For details about what specific functions have been proposed for Ambn, see "*Proposed fucntions of Ambn*".

Ambn sequence conservation

In searching for domains that control the functions of Ambn, it is useful to highlight what sequences and physicochemical properties of the protein are conserved across vertebrates with enamel. Conserved properties of Ambn include its richness in proline and glutamine residues and trio of putatively phosphorylated serine residues, both of which are features shared by other EMPs of the SCPP family [95], and its steep difference in isoelectric points between one end of the protein and the other [96], due to neutrally charged, hydrophobic amino acids in the N-terminal part and highly acidic amino acids in the C-terminal part [97]. The Y/F-x-x-Y/L/F-x-Y/F self-assembly motif is conserved across nearly all tetrapod species and was established via *in vitro* and mouse studies to be necessary for Ambn self-assembly and proper prismatic enamel formation [46]. Among species with functional prismatic enamel, Ambn residues that primarily reside in the N-terminal region (encoded by exons 2-6) display a high degree of conservation, and the variable region lies in the exons 6-, 7-, and 13-encoded segments [95]. Unchanged and conservative positions are subject to strong selection pressures indicating their functional significance. EMPs are subject to pseudogenization in the case of animals with non-functional dentition. Sloth, aardvark, and armadillo lack functional enamel and examination of their Ambn sequences have revealed numerous substitutions in conserved positions, premature stop codons, frameshifts in exon 13, and nucleotide substitutions at splice sites [95]. Such drastic changes suggest either an inactivation of the *Ambn* gene or a gene encoding a non-functional protein.

Proposed functions of Ambn

A range of functions have been proposed and supported for Ambn in enamel formation and ameloblast integrity. Ambn is a tooth-specific protein, and amongst its proposed functions is its role in the maintenance of rod-interrod morphology [69,98]. N-terminal Ambn proteolytic cleavage fragments selectively accumulate in the enamel sheath space [66], and Ambn has been colocalized with Amel along the boundaries of developing rods in mouse molars [99]. Disruptions in enamel prism formation in mouse models for mutant and overexpressed *Ambn* have demonstrated the importance of Ambn for prismatic structure (Table 2 and section "*Animal models*"). Small, short enamel crystals in transgenic *Ambn* mouse models reinforce the notion that Ambn is involved in controlling certain aspects of apatite mineralization [87,88]. The hypomineralized enamel in $Ambn^{G/G}$ model mice [46] indicated that self-assembly enables Ambn to guide HAP crystals into the correct, highly mineralized prismatic enamel structure.

In accordance with its putative role in enamel prism formation and maintenance, Ambn contains calcium-binding domains in its C-terminal region, which undergoes proteolytic processing by MMP-20 immediately after secretion. Peptides of the C-terminal region were found to accumulate on enamel rods [100], and its putative structure was predicted via *in silico* modeling of full-length Ambn [97]. Calcium binding was subsequently confirmed *in vitro* and found to be hampered by phosphorylation of Ambn and dependent on its oligomer formation [101,102].

Not only is Ambn implicated in organization of enamel crystals, but it is also involved in cellular functions. Ambn stimulated proliferation and adhesion of immortal mouse-derived periodontal ligament cells via the modulation of bone morphogenetic protein and type I collagen expression [103]. As further evidence of Ambn as a signaling molecule, it enhanced dentin formation and pulpal healing in the incisors of pulpotomy-treated miniature pigs [104]. Moreover, Ambn functions in non-dental tissues are supported. The presence of Ambn in the bone ECM is important for healing and prevention of long bone fractures [105], and Ambn and Amel appear to play growth factor-like signaling roles in

mandibular bone physiology [106]. Furthermore, Ambn was detected in various tissues of the human gastrointestinal tract [53].

The poorly formed enamel in *Ambn*$^{\Delta 5\text{-}6}$ mutant mice was associated with dysfunctional ameloblasts [91,92], indicating that Ambn sequences encoded by exons 5 and 6 are crucial for ameloblast cell function (Table 2). The roles of these exons are further discussed in section "Discovery of the amphipathic helix (AH) in Ambn: a probable key motif".

Protein-binding motif in Ambn – self-assembly and co-assembly

Both Amel and Ambn are known to self-assemble [70,107–110]. Amel self-assembles into ~20-nm-diameter nanospheres via its domains "A" and "B" [43]. The conserved 6-amino-acid Y/F-x-x-Y/L/F-x-Y/F peptide sequence appears twice in Amel domain "A." Moreover, Ambn self-assembles into ribbon or filament-like structures [70] via the Y/F-x-x-Y/L/F-x-Y/F motif at the N-terminal end of its region encoded by exon 5 [46]. Findings from our laboratory suggest that this same motif not only is responsible for its self-assembly but also leads to co-assembly with Amel [111].

Upon titrating recombinant Amel with increasing concentrations of a tryptophan-free variant of Ambn-derived AB2 peptide, representing the sequence encoded by exon 5 (Table 3), Su et al. [112] observed that the fluorescence spectra emitted by 3 tryptophan residues present in Amel showed a significant red shift, indicating a shift in those tryptophan residues to a more polar environment. However, no such change was observed when Amel was titrated with AB1 and AB6 peptides, which cover regions of Ambn that are N-terminal and C-terminal to the exon 5 sequence respectively (Table 3). Furthermore, upon measuring the circular dichroism (CD) of Amel in the presence of Ambn peptides, the percentage of α-helix in Amel increased with increasing concentration of AB2. Other Ambn peptides did not modify the secondary structure of Amel. These data provided first evidence for direct interaction between Amel and Ambn via the exon 5-encoded motif in Ambn. *In vivo* immunofluorescence analysis using fluorescence resonance energy transfer (FRET) verified that 17 kDa N-terminal fragments of Ambn accumulate in the rod-sheath space and colocalize with the tyrosine-rich Amel peptide (TRAP) fragments of Amel [99]. Immunofluorescence images also showed that Amel and Ambn co-localize within the cells and at the secretory front (Fig. 1, a&b) (protocol from [113]). The same N-terminal 45 residues of Amel (TRAP peptide) also interacted with Ambn *in vitro* [112].

A series of co-immunoprecipitation (co-IP) experiments were conducted to show direct binding of Amel and Ambn through the Y/F-x-x-Y/L/F-x-Y/F motif of Ambn [111]. Proteolytic fragments of Ambn and Amel eluted together as complexes from porcine enamel matrix protein extract when pulled down with either anti-Ambn or anti-Amel antibodies. Based on biophysical evidence from Su et al. [112] and colocalization of the proteins within developing enamel matrix [99,111,114], recombinant Ambn variants AmbnΔ5 and AmbnΔ6 were tested for co-IP with Amel. AmbnΔ6 co-precipitated with Amel, whereas AmbnΔ5 failed to bind to Amel. To further pinpoint the region within Ambn exon 5 that directly interacted with Amel, three Ambn peptides were passed through an Amel co-IP column. Peptide AB2N (Table 3), which contains the Y/F-x-x-Y/L/F-x-Y/F motif, co-eluted with Amel, while AB2C and AB2N-GGG with the 3 key amino acids of the Y/F-x-x-Y/L/F-x-Y/F motif mutated to glycine [46] failed to bind to Amel. These results confirmed that the Ambn Y/F-x-x-Y/L/F-x-Y/F motif is directly involved in its co-assembly with Amel within the enamel matrix.

Recent work from our laboratory elucidated how Ambn-Amel co-assemblies may affect enamel mineralization [110]. Atomic force microscopy (AFM), dynamic light scattering (DLS), and transmission electron microscopy (TEM) studies showed that the diameter of Amel nanospheres was not affected by lower concentrations of Ambn (from 1:100-1:5 Ambn:Amel ratio); however, the nanosphere diameter decreased significantly (from ~20 nm to ~7 nm) with increasing concentration of Ambn (Ambn:Amel ratios greater than 1:3). Ambn-derived AB2 peptide specifically affected the size of Amel self-assemblies, making them smaller, but AmbnΔ5 and AB4 peptide did not, supporting previous co-IP data [111]. The ability of Amel to stabilize ACP phase allowed controlled nucleation and growth of HAP within the enamel matrix [118]. Amel stabilized ACP for a longer time than Ambn alone at the same concentration [110]. Addition of Ambn to Amel even at low concentrations (Ambn:Amel ratio as low as 1:100) accelerated nucleation of HAP (ACP-to-HAP transition). Taken together with the co-assembly data, it is reasonable to suggest that changes in Ambn concentrations in the mineralizing enamel microenvironment could affect how long Amel stabilized ACP and allowed for its transition to HAP. These *in vitro* data together with the studies of *Ambn* engineered mouse models suggest that Ambn not only is involved in cell-matrix adhesion or signaling but also involved in HAP nucleation and enamel mineralization.

Cell-binding motifs in Ambn

The suggestion that Ambn may be implicated in ameloblast cell function, particularly adhesion, arose as a consequence of observations from *Ambn*$^{\Delta 5\text{-}6}$ model mice (Table 2 and [91]). In these mice, it was observed that although developing mouse molar ameloblasts initially appear normal, they begin to lose polarization and their attachment to

Table 3
Synthetic Ambn-derived peptides used for identification of the Amel-interacting motif of Ambn using co-immunoprecipitation (co-IP) [111]; for identification of the amphipathic helix (AH) motif of Ambn using circular dichroism (CD), tryptophan fluorescence spectroscopy, and synthetic membrane leakage assays [115] and cell culture experiments [116]; and for analysis of the interplay between the AH motif and the Amel-interacting motif using electron paramagnetic resonance (EPR) [117]. Amino acids of the AH in AB2 (peptide comprising the sequence encoded by exon 5), and xAB2N are italicized. Substituted amino acids in AB2N peptide variants [115] are italicized. Amino acids in AB2 and xAB2N mutated to cysteine and covalently tagged with a paramagnetic spin label [117] are underlined. Each of those peptides was spin-labeled at a single site, generating 3 xAB2N and 6 AB2 peptides, each with a spin label at one site, for EPR experiments.

Sequence	Exon(s)	Peptide name
^{27}VPAFPQQPGAQGMAPPGMASLSLETMRQLGSLQGLNALSQ^{66}	3 + 4	AB1
^{67}YS*RLGFGKALNSLWLHGLLP*PHNSFPWIGPREHETQQ^{103}	5	AB2
^{51}TMRQLGSLQGLNALSQYS*RLGFGKALNSLWLHGLLP*^{86}	C-terminus of 3 + 4 + N-terminus of 5	xAB2N
^{104}PSLQPHQPGLKPFLQPTAATGVQVTPQKPGPQPPMHPGQLPLQ^{146}	N-terminus of 6	AB4
^{147}EGELIAPDEPQVAPSENPPTPEVPIMDFADPQFPTVFQIAR^{187}	7 + C-terminus of 6	AB5
^{240}YGTLFPRFGGFRQTLRRLNQNSPKGGDFTVEVDSPVSVTKGPEK^{283}	13	AB6
^{87}PHNSFPWIGPREHETQQ^{103}	C-terminus of 5	AB2C
^{67}YSRLGFGKALNSLWLHGLLP^{86}	N-terminus of 5	AB2N
^{67}YS*D*LGFG*D*ALNSLWLHGLLP^{86}		AB2N-R69D/K74D
^{67}YSRLGFG*D*ALNSLWLHGLLP^{86}		AB2N-K74D
^{67}YSRLGFG*L*ALNSLWLHGLLP^{86}		AB2N-K74L
^{67}YSRLGFGKAL*K*SLWLHGLLP^{86}		AB2N-N77K
^{67}YSRLG*S*GKALNSLWLHGLLP^{86}		AB2N-F72S

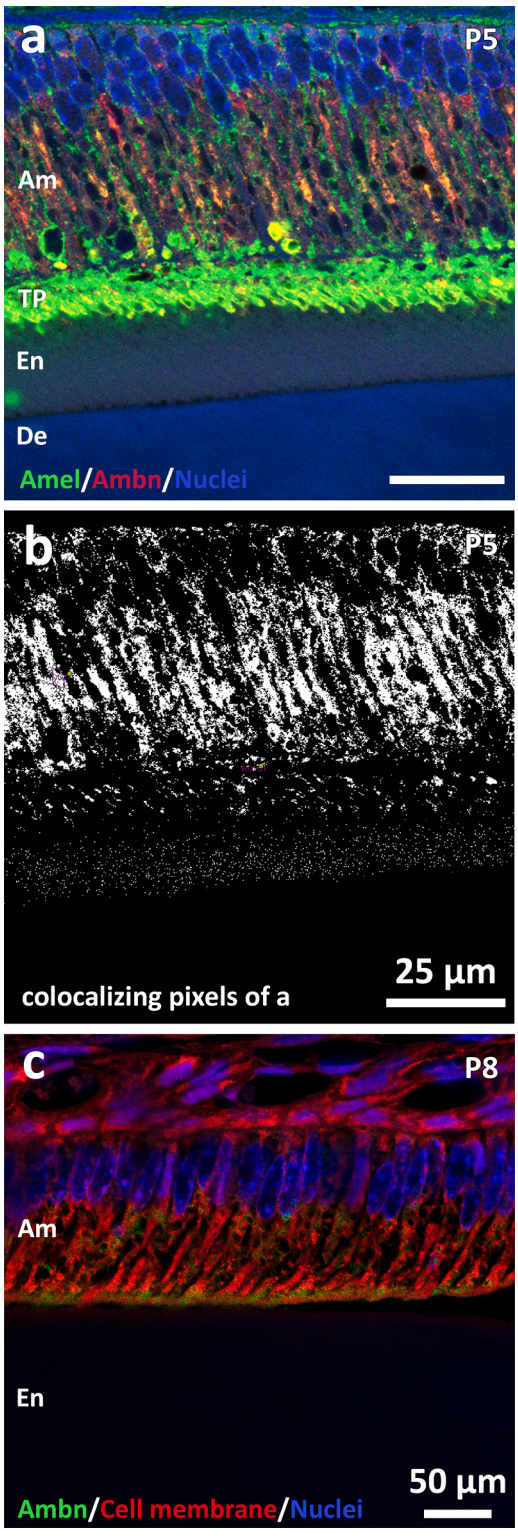

Fig. 1. **(a&b)** Confocal micrograph of postnatal day 5 (P5) incisor ameloblasts showing that Amel (green in **a**) and Ambn (red in **a**) colocalize at the secretory stage within the cells and at the secretory front (Tomes' processes). **(a)** Merged image, **(b)** colocalizing pixels of **a**. Am- ameloblasts, TP- Tomes' processes, En- Enamel, De- Dentin. Scale bar = 25 µm for both panels. **(c)** Confocal image of postnatal day 8 (P8) incisor ameloblasts showing Ambn (green) colocalizing with the ameloblast cell membrane (red) primarily at the secretory front of ameloblasts (Am). Scale bar = 50 µm. For more details on ameloblastin-membrane co-localization, see "*Ambn-cell surface colocalization*".

the enamel ECM beginning at secretory stage (P3) [91]. These dysmorphic cells then proliferate abnormally forming a multi-cell layer, with a complete loss of cell polarity (characterized by the position of the nucleus) and height. Based on the morphology of the cells and dysregulation in the expression levels of *Msx2, p27* and *p75*, the authors proposed that in the absence of normal Ambn, ameloblasts de-differentiate to an inner enamel epithelium like cell type.

In addition, Fukumoto et al. reported an increase in the adhesion of dental epithelial cells on recombinant Ambn-coated surfaces, with this behavior not extending to other epithelial (MDCK, HeLa), or fibroblast cell types [91]. Based on the collective observations of ameloblast pathology from mutant mice and the *in vitro* cell adhesive behavior, it was suggested that Ambn may play a direct role in the adhesion of ameloblasts to the developing enamel ECM [91,92,119].

Cell culture assays from several research groups identified motifs on Ambn that could mediate its adhesion of ameloblasts to the ECM. Unlike odontoblasts and osteoblasts, ameloblasts are unique ectodermal-derived cells that do not persist in fully developed enamel. After the maturation stage of amelogenesis, ameloblasts transform into short cuboidal cells of the reduced enamel epithelium which subsequently fuse with the oral ectoderm and are lost to the oral cavity upon tooth eruption [9]. Isolation of sufficient quantities of viable primary ameloblasts is challenging [120–124]; hence several immortalized ameloblast cell lines have been developed through the years (Fig. 2). These ameloblast-like cell lines have been shown to express EMPs at both the mRNA and protein levels and can induce mineralization in cell culture under certain conditions [125–130].

A previously identified heparin-binding VTKG motif (Fig. 3) on rat Ambn was identified as mediating Ambn cell-binding activity on dental epithelial, HAT-7 (Fig. 2), and SF2 cells [68,131]. Dental epithelial cells, HAT-7, and SF-2 cell lines adhered to recombinant rat Ambn-coated surfaces with the addition of heparin and heparan sulfate, selectively inhibiting attachment of dental epithelial cells [131]. The authors also report the presence of a heparin-insensitive cell-binding region in the N-terminal region of the protein. Subsequently, a fibronectin-binding motif was identified on exon 7 of rat Ambn [132] (Fig. 3). It was

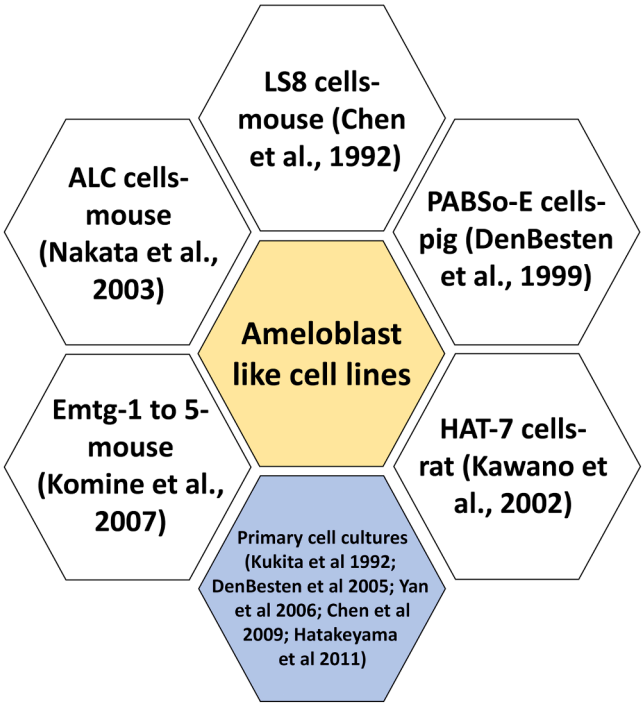

Fig. 2. Several immortalized ameloblast-like cell lines and primary cell cultures used by different investigators. We used ALC, Hat-7, and LS8 for our *in vitro* studies.

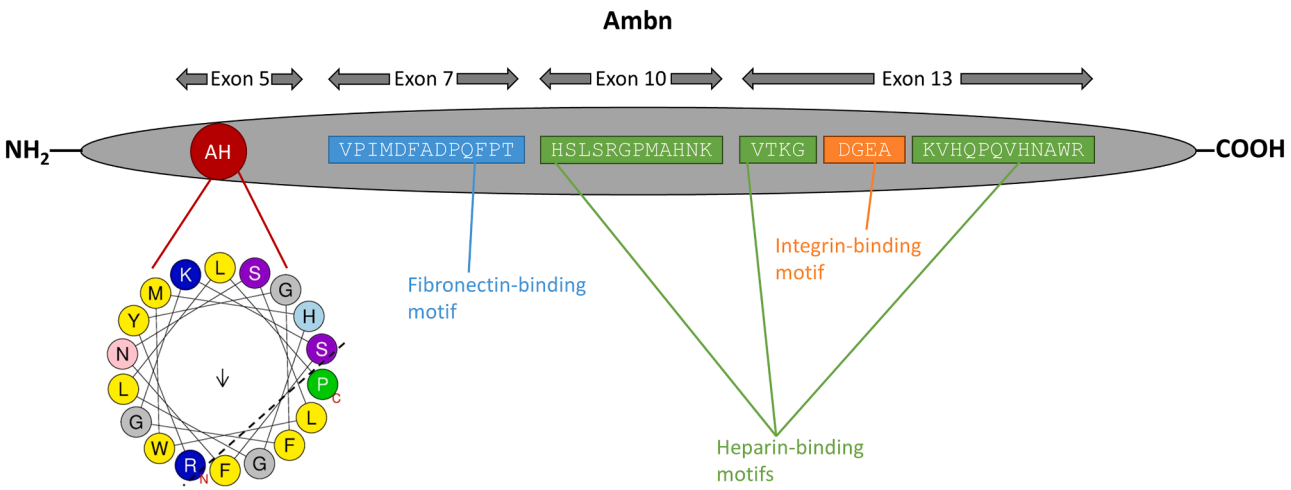

Fig. 3. Schematic illustration of reported integrin- [68], heparin- [131], and fibronectin-binding motifs [132] of Ambn as well as a putative membrane-binding amphipathic helix (AH) motif. The exons encoding these motifs are shown at top. The AH in human Ambn is composed of amino acids 64 to 81 and is plotted via Heliquest on a helical wheel with amino acids at bottom right to the dashed line comprising the hydrophobic face. Arrow designates direction of hydrophobic moment. Yellow: hydrophobic residues, blue: basic residues, pink and purple: polar residues, gray: glycine, green: proline. Quantities for hydrophobic moment, hydrophobicity, and net charge are listed in [116]. For details on the discovery of the AH motif see section below.

demonstrated that exon 7-encoded region of rat Ambn promoted the adhesion of osteoblast and fibroblast cells through these 13 amino acid-long motifs. Either the deletion of this motif or a single amino acid substitution of an aspartate residue resulted in a complete loss of cell-binding activity. The proposed mechanism of cell binding was through secreted fibronectin mediating the adhesion by binding to the fibronectin motif of Ambn on one side and cell surface receptor integrins on the other. Using a yeast two-hybrid (Y2H) system, Ambn was found to potentially interact with Cd63, a transmembrane glycoprotein from the tetraspanin family [133]. In support of this, Ambn could be immunoprecipitated with Cd63 in SaOS2 cells engineered to overexpress Ambn protein [134]. The addition of anti-Cd63 or anti-integrin β-1 antibody has been shown to result in a neutralization of Ambn cell adhesive effects on periodontal ligament cells in culture [135]. Molecular dynamics simulation of human and mouse Ambn identify complex Cd63-binding sites on Ambn sequences of both species [136].

Discovery of the amphipathic helix (AH) in Ambn: a probable key motif

Analysis of site-specific selection constraints and conserved domains within Ambn-coding sequences from 56 different mammalian species revealed that most of the conserved amino acid residues are confined to the N-terminal region of Ambn encoded by exons 2 through 6, suggesting that these positions are subject to a high functional constraint [95]. The VTKG heparin-binding motif is present only in kangaroo, rat, mouse, and hamster and was suggested to have evolved secondarily during rodent evolution. The DGEA integrin-binding motif is present only in mouse, rat and hamster within rodents and is exclusive to murid evolution [95]. A systematic amino acid sequence analysis of Ambn from 47 species belonging to multiple classes within vertebrates further supported the low sequence conservation of the heparin-, fibronectin-, and integrin-binding motifs, and identified a highly conserved new amphipathic helix (AH)-forming motif residing within the region encoded by exon 5.

The AH motif in Ambn is composed of 18 amino acid residues that form a helix with a polar (hydrophilic) and a hydrophobic face and is highly conserved across mammals. The version of this AH motif that appears in the human Ambn sequence is plotted in Fig. 3 on a helical wheel via Heliquest, an *in silico* method to predict formation of specific helical structure types [137]. Hydrophobic residues are lined up adjacent to one another (marked by the dotted line in Fig. 3) to form the hydrophobic face oriented away from the polar and charged (basic) residues. The presence of an AH-forming motif was identified by sequence analysis as being unique to Ambn and was not present in Amel or Enam sequences from human, pig, or mouse [116].

AH motifs have previously been identified in a variety of other proteins and peptides and frequently take shape upon direct interaction between the AH-forming region and a phospholipid membrane, resulting in an α-helical wedge inserted parallel to the membrane bilayer between phospholipid head groups [138]. Typically, AH-forming regions contain polar amino acids every three to four residues and hydrophobic amino acids every three to four residues. This alternating pattern, once the helix is formed, allows the polar side chains to line up and face the solvent while nonpolar side chains also line up and are buried among the phospholipid acyl chains—an energetically favorable structure that imparts amphipathicity (alternatively called amphiphilicity) to the helix [139]. This lining up of side chains is illustrated in Fig. 3 for the AH motif in Ambn. The ability of protein motifs to form AH structures facilitates their functions in a variety of physiological contexts, including but not limited to antimicrobial defense [140], lipid droplet coating, protection of membranes against temperature extremes, and organelle biogenesis aided by membrane curvature and sensing [138].

Binding of Ambn to phospholipid bilayers via its AH motif – a synthetic model

In order to test for Ambn-membrane interactions, recombinantly expressed mouse Ambn was combined with synthetic liposomes, also known as large unilamellar vesicles (LUVs), made to mimic epithelial cell membranes [115]. Ambn was found by fluorescence spectroscopy to experience a blue shift in the fluorescence emission peak of its tryptophan residues upon addition of LUVs, indicating a change to a more hydrophobic microenvironment surrounding Ambn tryptophan residues. Ambn also induced leakage of LUV contents and clearance of LUVs into smaller particles. Cryo-TEM also showed deformation of LUVs upon addition of Ambn. All these results—tryptophan fluorescence blue shift, LUV leakage and clearance, and visible deformation of LUVs—are known to indicate interaction of an agent with membranes. CD spectra of Ambn showed more α-helical content in the protein in the presence of LUVs than in their absence. Recombinant deletion mutants of Ambn were expressed to test the hypothesis that a motif located in the exon 5-encoded region, where bioinformatics had predicted an AH, was

causative of helix-mediated membrane interactions. Ambn with deletion of the sequence encoded by exon 5 (AmbnΔ5) failed to form an α-helix in the presence of LUVs and caused significantly less leakage and clearance when added to LUVs than did Ambn-WT, while Ambn with deletion of the sequence encoded by exon 6 (AmbnΔ6) formed an α-helix and leaked and cleared LUVs similarly to Ambn-WT.

To further identify which regions of Ambn interact with membranes, a range of peptides were designed and synthesized (Table 3). Whereas AB2, composed of the 37-amino-acid sequence encoded by exon 5, induced LUV leakage and experienced a coil-to-helix transition when mixed with LUVs, AB1, AB4, AB5, and AB6 (representing sequences encoded by exons other than exon 5) induced significantly less leakage and remained in a random coil conformation. Smaller peptides each comprising either the N-terminal 20 amino acids (AB2N) or the C-terminal 17 amino acids (AB2C) of AB2 (encoded by exon 5, Table 3) were also tested. Only AB2N caused LUV leakage, formed a helix on LUVs, and underwent a blue shift in its tryptophan fluorescence peak. Amino acids 3 through 20 of this peptide were bioinformatically predicted to comprise an AH motif.

The reliance of AB2N-membrane interactions on AB2N amphipathicity was tested by synthesizing AB2N peptide variants each carrying one- or two-point substitutions that perturbed charge or hydrophobicity (Table 3). Biophysical experiments showed that the two mutations, R69D/K74D and K74D, that most decreased the charge of the peptide had the greatest negative effect on membrane interactions. F72S, which preserved the positive net charge of AB2N but eliminated its hydrophobic face, compromised its ability to form a helix on LUVs and cause LUV leakage but preserved the blue shift in its tryptophan fluorescence peak in the presence of LUVs. Thus, to varying extents, loss of electrostatic charge or hydrophobicity of the N-terminal residues encoded by *Ambn* exon 5 costs the ability of the region to interact with membranes. Alternating charge and hydrophobicity being the definition of an amphipathic character, it was concluded that AB2N, as well as the region within Ambn that it represents, forms an AH in the presence of LUVs that cannot properly bind membranes without its amphipathic character.

Binding of AH motif to cell surfaces

From the support for an *Ambn* AH motif generated by the above experiments using LUVs emerged the hypothesis that a functional AH motif is necessary for Ambn to interact with the ameloblast cell surface. Our research group then tested this hypothesis by first using *in vivo* colocalization analysis of Ambn and the ameloblast cell membrane [116].

Ambn-cell surface colocalization

Immunofluorescence analysis of Ambn and a membrane-labeling dye (DiD) in wild-type (WT) postnatal day 8 (P8) developing mouse incisors revealed that Ambn colocalized with the ameloblast cell membrane at the interface of the enamel matrix and ameloblasts (Fig. 1c). Recombinant mouse Ambn labeled with FITC and incubated with ALC, LS8, and NIH3T3 cells resulted in a selective immunolocalization of Ambn on the cell processes compared to transferrin (which bound to the cell surface in a uniform manner) and lysozyme (negative control) [116].

Ambn AH-cell interactions in 2-D cell culture

We then used ameloblast-like cell lines LS8 and ALC to examine interactions of the Ambn AH with ameloblast cell surfaces in 2-D cell culture models (Fig. 2). A series of Ambn-derived peptides (AB1-AB6, AB2C, and AB2N from Table 3) and Ambn recombinant proteins including WT and mutants were designed for cell attachment and spreading assays. ALC, LS-8, and NIH3T3 cells were cultured on recombinant WT-Ambn-coated plates in the presence of competing test and control peptides and proteins, and their effect on inhibiting cell adhesion and spreading was examined [116]. On an Ambn-coated surface, AB2 displayed the strongest inhibition of cell attachment and spreading in all three cell types compared with peptides from other regions of Ambn suggesting the presence of a functional membrane binding motif. Removal of the exon 5-encoded region of Ambn (AmbnΔ5) resulted in a loss of this inhibitory effect compared to WT recombinant Ambn. AB2N peptide alone could sufficiently replicate the effect of AB2, while AB2C was incapable of doing so independently. Two additional recombinant Ambn proteins were used, in which the AH motif was disrupted either through a deletion of the 20 N-terminal amino acid residues out of the 37 residues encoded by exon 5 (AmbnΔ5N) or inactivation of the polar face of the AH through the double substitution R69D/K74D (Ambn-R69D/K74D). Both disruptions to the AH resulted in the loss of competitive inhibition of cell attachment and a more diffuse protein distribution on the surface of ALC in immunofluorescence.

AH motif-cell interactions in 3-D cell culture: polarity, elongation

A modified 3-D-on-top type culture was developed that allowed to create an asymmetrical microenvironment with proteins being present only along one side of the cells [141]. This cell culture model was used to examine the role of Ambn AH motif in the establishment of ameloblast cell polarity and elongation.

Epithelial cell polarity – initiation and spatial cues

In epithelial cells including secretory-stage ameloblasts, polarity (structural and functional asymmetry) is a characteristic feature and is critical for normal functioning, as epithelial cells are involved in the transport of ions, nutrients, and secretion. Epithelial cell polarity is reflected in the positioning of the distinct membrane proteins, cytoskeletal components, nucleus, and intracellular organelles. As a result, there are three distinct membranes in an epithelial cell: the apical contact-free, basolateral contacting, and lateral membranes [142].

Polarity is initiated by an external signaling mechanism in which cell-cell and cell-matrix interactions play important roles [143]. Cell-cell contacts are mediated by a calcium dependent superfamily of adhesion receptors—the cadherins. Calcium is essential for both the generation and the maintenance of E-cadherin-mediated epithelial cell-cell adhesion and polarity [144,145]. Mature E-cadherin contains a single transmembrane domain, a cytoplasmic domain, and an ectodomain [146]. The extracellular domain of cadherins cluster with one another in a calcium-dependent manner, forming homotypic interactions. However, this lateral clustering is weak and a strong interaction develops only following the cytoplasmic domains binding with their interacting proteins—primarily the catenins [143].

The cadherin cytoplasmic interaction proteins include those that are related to regulating its turnover (p120 catenin, Hakai) and those that link it to the actin cytoskeleton (α- and β-catenin) [147,148]. Conditional ablation of β-catenin in ameloblasts has been shown to result in enamel mineralization defects, including a disruption of the prismatic microstructure (attributed to disrupted ameloblast cell migration) and loss of ameloblast elongation and polarization [149]. *Keratin-14Cre* driven deletion of p120 catenin in ameloblasts results in a loss of ameloblast polarization and morphology and impacts enamel mineralization [150]. Additionally, MMP-20 facilitates ameloblast lateral cell movements by cleaving E-cadherin on ameloblasts [151,152].

Once cell polarity is initiated, it is maintained by the organization of polarity proteins into the apical or basolateral membranes resulting in distinct membrane complexes that reinforce the asymmetry [153,154]. Assembly of tight junctions occurs rapidly after the establishment of cell-cell contacts, and this functions to demarcate the apical and basolateral membrane domains [155]. In polarized rat secretory stage ameloblasts, the proximal ameloblast cell membrane labels intensely with the apical membrane domain protein Par-3 and the distal membrane with tight junctional protein claudin-1 [156]. Rho-associated coiled-coil protein kinases ROCK-1 and ROCK-2 have been shown to be vital for the

development of ameloblast cell polarity, with their absence resulting in a loss of polarized distribution of E-cadherin and β-catenin in ameloblasts [157]. We selected a few markers described above to demonstrate Ambn-mediated polarity in our newly developed 3-D cell culture system.

Ambn promotes ameloblast cell polarization and morphological changes in 3-D via the AH motif

Recombinant mouse Ambn and Amel induced the formation of 3D clusters of ameloblast lineage cells (ALC, LS-8, and HAT-7) without the aid of additional growth factors as observed with growth factor-reduced Geltrex, type I collagen, and gelatin gels [141,158,159] (Fig. 2). The cells within the clusters exhibited a selective elongation along the Z axis resulting in increased height/width aspect ratios that were 7 times greater than those of planar cells in the control (aspect ratio < 1). Recombinant mouse Ambn induced this change more effectively in the cells at lower concentrations (0.36 μM) compared to Amel (0.99 μM), with a strong correlation between the concentration of Ambn in the substrate and cell elongation ($R^2 = 0.85$). This effect of Ambn was recapitulated using both enamel matrix extract from developing porcine molars and recombinant Ambn 17 kDa cleavage fragment protein.

Similar to observations in ALC cells, HAT-7 cell clusters, formed with Ambn 17 kDa fragments, displayed a polarized distribution of Par-3 protein at the nascent cell-cell junctions (Fig. 4a-c). Par-3 localized at the ameloblast cell membrane distal to the nucleus while actin immunolabeling was uniform throughout the entire outline of the cells, further highlighting the polarity in Par-3 distribution (Fig. 4, a&b). Tight junctional protein claudin-1 (cldn1) was also asymmetrically distributed, immunolocalizing along the same pole of the cell as Par-3 (Fig. 4d-f).

The bioactive region within Ambn responsible for this cell behavior was identified to be the exon 5+6 region using recombinant Ambn mutants AmbnΔ5 and AmbnΔ6. Removal of the exon 5-encoded region or heat-denaturing Ambn resulted in failure to cluster, elongate, or polarize the cells, while exon 6 deletion had a milder effect in comparison. Two dimensional (2D) monolayer cultures of LS-8 cells treated with Ambn displayed an upregulation in the gene expression levels of planar cell polarity protein Vangl2 (2.8 times) and cell polarity protein Par-3 (3.8 times) compared to control cells treated with heat denatured Ambn and AmbnΔ5 [160].

Taken together, the results suggest that Ambn may play a key role in mediating cell-cell and cell-matrix interactions during the initial stages of amelogenesis and this is predicated on the presence of a functional AH-forming motif within the exon 5-encoded region.

Ambn AH motif co-emerged with prismatic enamel

The novel AH motif supportably plays a significant role in prismatic enamel development. This argument follows from the fact that the motif is present only in mammalian Ambn [115], and mammalian enamel is a synapomorphy [20,22]. Considering the above observations, our research group hypothesized that the Ambn AH motif is correlated with the emergence of prismatic enamel by either directly or indirectly controlling the formation of ameloblast Tomes' processes [160].

We analyzed 53 vertebrate species for the presence of the AH-forming motif, and the AH motif was identified in 33 of the 42 mammals examined. Within these 33 mammals that contain the AH motif, 30 of them were observed to have a prismatic enamel microstructure (based either on direct observation, or inference from other species in the same

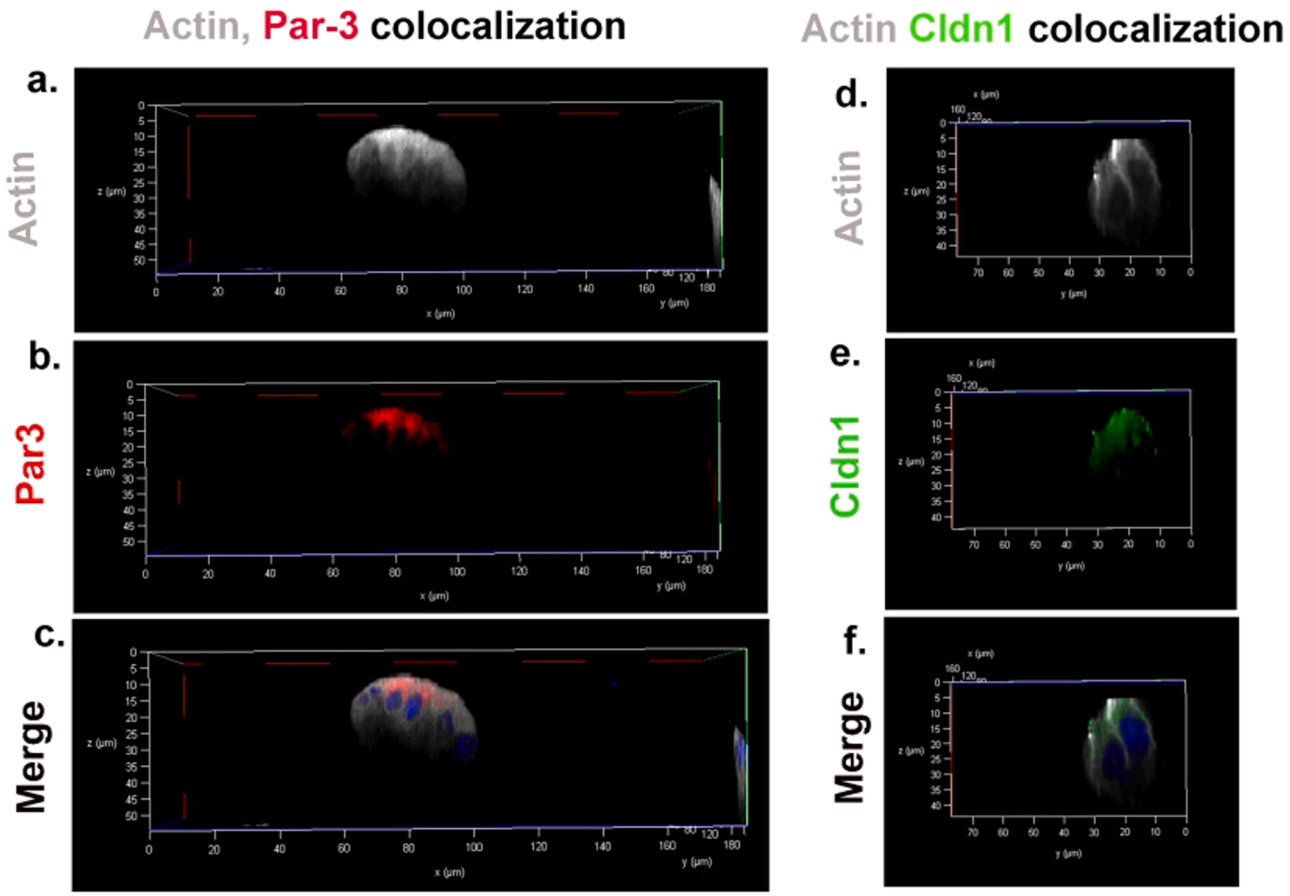

Fig. 4. Immunolocalization of Par-3 **(a-c)** and claudin-1 **(d-f)** with actin within HAT-7 cell clusters. **(a-c)** Axial sections from three-dimensional HAT-7 cell clusters with anti-actin antibody (grey pseudo color) reveal actin labelling the entire cell outline while Par-3 (red) is restricted basal to nucleus. **(d-f)** Tight junctional protein claudin-1 (cldn1) (green) also displaying a polarized distribution within HAT-7 cells labelled with actin (grey pseudo color) in axial sections.

genus) [160].

There are exceptions to this observed correlation between the presence of an AH motif and prismatic enamel in mammals. Among them, the gray short-tailed opossum (*Monodelphis domestica*) and cape elephant shrew (*Elephantulus edwardii*) have a prismatic enamel structure but are predicted not to form a helix due to an intervening proline residue in the middle of the AH motif. Peptides derived from AH sequences of *M. domestica* and *E. edwardii* could effectively insert into the lipid bilayer of LUV membranes (in leakage assays) and inhibit the attachment and spreading of ALC and LS-8 cells on recombinant Ambn-coated plates. This suggests that these species do form a functional AH despite the intervening proline residue [160].

Within mammals, the only species that contains an AH motif without accompanying prismatic enamel are whales. The whales examined, however, were either enamel-less (*Metapenaeus monoceros* and *Physeter macrocephalus*) or edentulous (*Balaenoptera acutorostrata scammoni*) and were hence considered irrelevant to the correlation. In non-mammalian vertebrates (reptiles, amphibians, sarcopterygians excluding tetrapods, and actinopterygians), the AH motif is absent and the enamel in these species is aprismatic in structure. Peptides derived from species that can neither form a helix, nor have prismatic enamel, like that of *Xenopus laevis* (amphibian), *Alligator mississippiensis* (reptile), and *Dasypus novemcinctus* (mammal), were unable to effectively inhibit the spreading of ALC and LS-8 cells on Ambn-coated plates, suggesting the absence of a membrane interaction domain in the Ambn of these species.

Further support for the correlation between AH and prismatic enamel can be found in the observations from platypus (*Ornithorhynchus anatinus*). Ambn from *O. anatinus* contains the AH motif, and in this species although adults don't have enamel, a partly prismatic enamel structure has been reported in the case of juveniles [161,162]. This suggests that Ambn in this species may play a role in the development of prismatic enamel in juveniles.

Overall, through a combination of experimental evidence and *in silico* sequence analysis, 86.3 % of the total species examined (51 species) supported the correlation between the presence of a functional AH motif in Ambn and prismatic enamel. Additionally, it was found that the correlation could be expanded beyond the species examined in this study. Species with sequences identical to peptides derived from AH motifs have prismatic enamel and, in turn, species with sequences identical to the synthetic peptides derived from equivalent regions without AH lack prismatic enamel.

A proposed multitargeting domain encompasses the AH motif

The Y/F-x-x-Y/L/F-x-Y/F motif [46], which spans residues 67 through 72, and the AH motif, which spans residues 69 through 86 of the mouse Ambn sequence [115], share four residues. This overlap introduces the question of competition between Ambn self-assembly or co-assembly and Ambn-membrane interactions. The failure of sequences from other regions of Ambn to interact with membranes [115] or with Amel [110,111] leaves this short stretch of residues to reconcile two or more types of interactions that differ greatly in structural nature. Our research group sought to identify locations in the Ambn sequence where residues participated in each interaction [117]. We hypothesized that the self- and co-assembly motif and the AH motif were part of a larger multitargeting domain, enabling the multifunctionality of Ambn.

Electron paramagnetic resonance (EPR) with site-directed spin-labeling (SDSL) is a powerful biophysical technique that unveils structural changes at the level of individual amino acid residues [163]. It was thus employed to locate structural changes in residues of Ambn peptides upon interactions with Amel protein, Ambn protein, and LUVs mimicking cell membrane [117]. Peptides AB2 and extended AB2 N-terminus (xAB2N), whose sequence encompasses that of AB2N and 16 residues N-terminal to it in the mouse Ambn sequence, were individually spin-labeled (Table 3). The resulting EPR spectra revealed increases in secondary structure formation for all labeled residues in both peptides except for residue 35 in AB2 (equivalent to residue 101 in Ambn) in the presence of LUVs. In the presence of Amel or Ambn protein, EPR revealed increases in structure formation for all sites (including AB2 residue 35). Spin-labeled peptides did not display a change in EPR spectra in the presence of BSA as a negative control.

At high concentrations of Amel, an additional feature arose in EPR spectra from labeled Ambn peptides, namely a "bump" to the left of the leftmost major spectral peak. This "bump" denotes a gain in tertiary/quaternary contacts, which is evidence of self- or co-assembly as it involves a peptide or protein interacting with another or with itself. Since this spectral feature is noticeably absent when LUVs are added to peptides, it was utilized to determine what interactions were taking place in three-component experiments, in which spin-labeled Ambn peptide, LUVs, and Amel were all present at once. When Amel was added first to the peptide, followed by LUVs, the tertiary/quaternary contacts appearing upon the introduction of Amel were greatly reduced upon addition of LUVs, signifying a loss of peptide-protein contacts and an accommodation of the evidently preferred membrane-bound state. The feature indicating peptide-protein contacts did not appear when Amel was added to peptide that was already mixed with LUVs. Therefore, it was concluded that Ambn-membrane and Ambn-Amel interactions, and most likely Ambn-Ambn interactions, are dynamic rather than static and compete with one another, with Ambn-membrane interactions appearing to dominate. Tryptophan fluorescence assays corroborated that changes observed in Ambn peptide because of interaction with Amel were attenuated if LUVs were present before addition of Amel. Furthermore, changes observed in Ambn peptide as a result of interaction with LUVs were similarly weakened by this measurement if Amel was present before addition of LUVs.

Given that EPR data showed residues beyond the Y/F-x-x-Y/L/F-x-Y/F motif to partake in self- and co-assembly and residues beyond the AH motif to interact with LUV membranes, the data support the existence of a larger multitargeting domain within Ambn. This domain encompasses both the AH and self-assembly motifs along with residues N-terminal and C-terminal to them. A schematic model for the function of this multitargeting domain in amelogenesis is presented in Fig. 5. The multitargeting domain of Ambn in the developing enamel matrix space dynamically interacts with the apical membrane of ameloblasts via the AH while also dynamically assembling and disassembling with other Ambn fragments and Amel fragments (Fig. 5). In this way the multitargeting domain of Ambn imbues it with a "two-handedness" that facilitates its ability to adhere ameloblasts via their apical membranes to the matrix and anchors its signaling functions.

Conclusions and perspectives

Ambn performs a plethora of functions via various domains, including those with post-translational modifications, protein-protein interactions, and calcium binding. Our recently identified multitargeting domain encompassing AH and self/co-assembly motifs encoded by *Ambn* exon 5 adds to the list of Ambn functional domains. While calcium-binding domains enable Ambn to regulate mineralization, the multitargeting domain most likely informs its direct effects on ameloblasts. We suggest that AH formation by residues within the multitargeting domain facilitates direct interaction between Ambn and cell membranes and at least partly accounts for the role of Ambn in adhering ameloblasts to the enamel-forming matrix. Given the high evolutionary conservation of the AH motif compared to the heparin- and integrin-binding motifs and its presence in 34 out of 37 mammalian Ambn sequences [115], direct membrane interaction via an AH motif may be the dominant mechanism for the cell adhesion role of Ambn. We hypothesize that, during amelogenesis, Ambn AH motif cooperates with the other cell binding motifs to regulate ameloblast cell adhesion to the matrix and is involved in cell polarity and the formation of Tomes' processes.

Induction of ameloblast polarization during secretory stage in

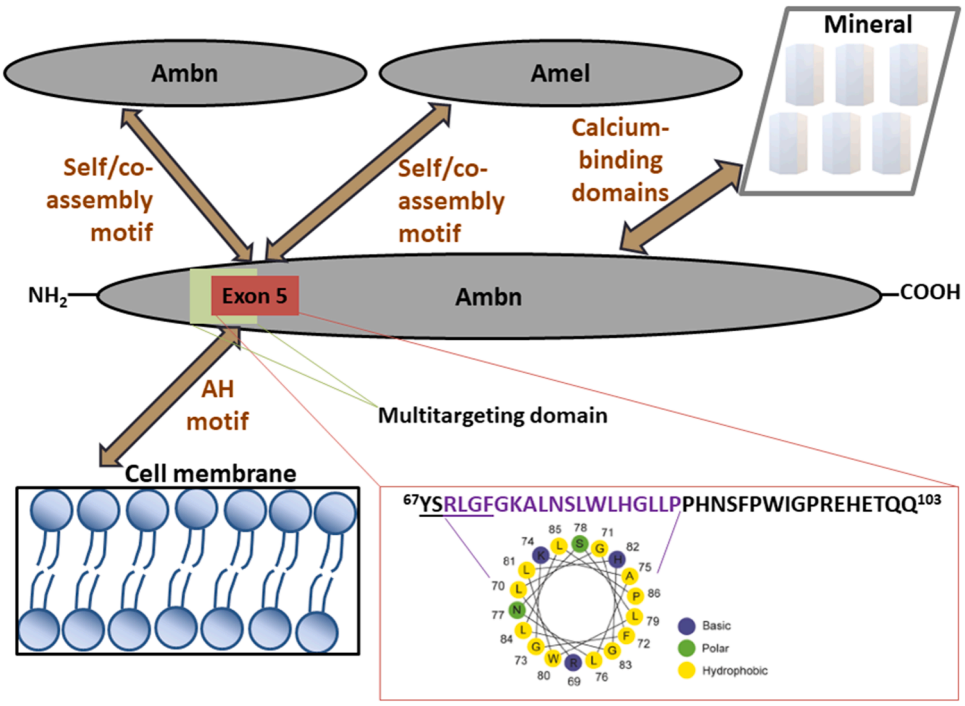

Fig. 5. Schematic of a proposed mechanism enabling the multitargeting domain of a single Ambn molecule to interact simultaneously with the plasma membrane of an ameloblast and with Amel or Ambn in the enamel-forming matrix. This domain is estimated to range from amino acids 57 to 90 of mouse Ambn (green rectangle). The AH motif, amino acids in purple in the inset, forms the structure schematized in the helical wheel to bind the membrane. Overlapping with the N-terminus of the AH, the Y/F-x-x-Y/L/F-x-Y/F motif, underlined in the inset, remains in proximity to the membrane while interacting with the corresponding motif of an Amel or other Ambn situated in the matrix, thus two-handedly tying the cell membrane to the matrix, and thus possibly carrying out the anchoring and polarization functions of Ambn. Calcium-binding domains in the C-terminal region mediate enamel mineral formation.

mammals leads to formation of Tomes' processes, which has been linked to prismatic structure as a mammalian synapomorphy [20]. Ambn induced the elongation and polarization of ameloblast lineage cells in 3D culture and upregulated gene expression levels of *Par-3, ROCK-1, ROCK-2, Vangl1*, and *Vangl2*, which are involved in regulating cell polarization. Moreover, Ambn selectively immunolocalized to ameloblast Tomes' processes *in vivo* on wild-type mouse secretory ameloblasts. Based on these collective observations, we propose that the Ambn AH motif may have evolved to function in signaling ameloblasts to generate Tomes' processes, and in turn establish a prismatic enamel architecture in mammals [116,159,160].

It should be noted that the above hypotheses do not exclude the possibility that during amelogenesis Ambn may interact with ameloblasts via receptors and other basement membrane components. Ambn might also interact with other adhesion proteins to enhance their binding to ameloblast membrane. Expression and localization studies on laminin-5 suggest that it adheres dental epithelial cells to the enamel matrix across stages of amelogenesis [164], and Ambn may well be involved in these interactions, assisting the adhesion function. These interactions could take place via the multitargeting domain and could define Ambn as a matricellular protein. Upon their secretion into the ECM, matricellular proteins do not essentially comprise the structure of the ECM, but interact with both structural and functional proteins, including receptors [165–167].

The interactome of Ambn warrants exploration and could account for the diversity of phenotypes among *AI* patients with mutated *AMBN* alleles. From loss of enamel prismatic structure to a complete loss of enamel, different mutations on *AMBN* and even the same mutation have differentially affected enamel in *AI* cases. Different mutations, or even the same mutation against a different background of polymorphisms in amelogenesis-related genes, could upset the delicate balance among various functions of Ambn in different directions. The sequence of the Ambn multitargeting domain and the competition between Amel or Ambn and the cell membrane for interaction with this domain could serve as regulators of this delicate balance in the multifunctionality of Ambn. For example, EPR spectra from the Ambn peptide/Amel/LUV three-component system suggest Ambn-membrane interactions to take precedence over co-assembly with Amel [117], which could be instrumental in keeping Ambn anchored to ameloblasts. Conversely, Amel could also, via its competition for interaction with membrane-bound Ambn, prevent it from remaining membrane-bound. The smaller increase in cell elongation induced by both Amel and Ambn, when compared to that induced by Ambn alone, supports the notion that Amel competes for Ambn in interaction with cell membrane [159]. Thus, it would make sense that mutations that alter the multitargeting domain of Ambn would cause a different phenotype from those that change the sequence elsewhere, and that polymorphisms in *AMEL* would theoretically modify the effect of *AI*-associated *AMBN* mutations on phenotype, given that Ambn and Amel functions appear to be intertwined.

The evolution of *AMEL* and *AMBN* supports the close relationship and similarities between their functions. *AMEL* and *AMBN* are paralogs of one another and of *ENAM*, as *AMEL* evolved from *AMBN*, which emerged from a duplication of *ENAM* [168]. Amel is also an intrinsically disordered protein having multiple functions and interactions with multiple partners [169], including Enam [170,171], CD63 [172], lysosome-associated membrane protein-1 (LAMP1) [173], and HAP crystals [174]. Like Ambn, Amel interacts with membranes with a concomitant increase in protein structural order [175,176]. It has been observed to shape-shift *in vitro* depending on pH, temperature, and solvent hydrophobicity [169]. Such conformational changes are hallmarks of intrinsic disorder, which is likely to imbue Amel and Ambn with their multifunctionality and propensity to be regulated by their environment and binding partners. Perhaps Ambn regulates Amel function by a dynamic mechanism mirroring that by which Amel appears to tune Ambn-membrane interaction. The multifunctionality of Amel also appears to inform the diversity of *AI* phenotypes associated

with *AMEL* mutations [177].

In summary, a body of research has uncovered the multifunctionality of Ambn, which is mediated by several motifs throughout the sequence but appears to center on the multitargeting domain in its N-terminal region. This domain controls the balance between Ambn self/co-assembly and its interaction with cell membranes, plays direct roles in cell-matrix adhesion and cell polarization, and could imbue it with the properties of a matricellular protein. *AI* cases associated with *AMBN* mutations are highly diverse and reflect its many functions. While most animal models obliterate or exaggerate Ambn expression and thus do not pinpoint its exact functions, *in vitro* and cell studies have illuminated possible mechanisms, and more recent and future animal models will evaluate the validity of and lend more perspective on those mechanisms.

Declaration of competing interest

The authors declare that they have no known competing financial interests or personal relationships that could have appeared to influence the work reported in this paper.

Data availability

Data will be made available on request.

Acknowledgements

Funded by NIH-NIDCR grants: R01DE013414 and DE027632 to J.M.-O. We would like to thank Mr. Thach-Vu Ho and Dr. Jingtan Su from the Center for Craniofacial Molecular Biology for technical assistance and valuable input.

References

[1] C.E. Smith, Cellular and chemical events during enamel maturation, Crit. Rev. Oral Biol. Med. 9 (2) (1998) 128–161.
[2] R.S. Lacruz, et al., Dental enamel formation and implications for oral health and disease, Physiol. Rev. 97 (3) (2017) 939–993.
[3] C. Robinson, et al., Chemistry of mature enamel, in *Dental Enamel: Formation to Destruction*, CRC Press, Boca Raton, FL, 2017, pp. 167–191. C. Robinson, J. Kirkham, and R.C. Shore, Editors.
[4] E. Beniash, et al., Transient amorphous calcium phosphate in forming enamel, J. Struct. Biol. 166 (2) (2009) 133–143.
[5] A. Boyde, Microstructure of enamel, Ciba Found. Symp. (1997) 20518–20527, discussion 27-31.
[6] A. Akasapu, U. Hegde, P.S. Murthy, Enamel surface morphology: an ultrastructural comparative study of anterior and posterior permanent teeth, J. Microsc. Ultrastruct. 6 (3) (2018) 160–164.
[7] J.D. Bartlett, Dental enamel development: proteinases and their enamel matrix substrates, ISRN Dent, 2013 2013684607.
[8] S.R.P. Line, P.D. Novaes, The development and evolution of mammalian enamel: structural and functional aspects, Braz. J. Morphol. Sci. 22 (2) (2005) 67–72.
[9] A. Nanci, Ten Cate's Oral Histology: Development, Structure, and Function, Elsevier Health Sciences, 2017.
[10] G.A. Macho, Y. Jiang, I.R. Spears, Enamel microstructure–a truly three-dimensional structure, J. Hum. Evol. 45 (1) (2003) 81–90.
[11] C. Robinson, J. Kirkham, R.C. Shore, Dental Enamel: Formation to Destruction, CRC Press, Boca Raton, FL, 2017.
[12] A. Nanci, H. Warshawsky, Characterization of putative secretory sites on ameloblasts of the rat incisor, Am. J. Anat. 171 (2) (1984) 163–189.
[13] S. Risnes, et al., TEM observations on the ameloblast/enamel interface in the rat incisor, Connect. Tissue Res. 43 (2-3) (2002) 496–504.
[14] S. Habelitz, Materials engineering by ameloblasts, J. Dent. Res. 94 (6) (2015) 759–767.
[15] A. Boyde, The development of enamel structure, Proc. R. Soc. Med. 60 (9) (1967) 923–928.
[16] S. Risnes, Growth tracks in dental enamel, J. Hum. Evol. 35 (4-5) (1998) 331–350.
[17] S. Nishikawa, T. Kawamoto, Planar cell polarity protein localization in the secretory ameloblasts of rat incisors, J. Histochem. Cytochem. 60 (5) (2012) 376–385.
[18] J.C. Hu, et al., Enamel formation and amelogenesis imperfecta, Cells Tissues. Organs 186 (1) (2007) 78–85.
[19] P.M. Sander, Prismless enamel in amniotes: terminology, function, and evolution. Development, Function, and Evolution of Teeth, Cambridge University Press, 2000, pp. 92–106.
[20] C.B. Wood, E.R. Dumont, A.W. Cromption, New studies of enamel microstructure in Mesozoic mammals: a review of enamel prisms as a mammalian synapomorphy, J. Mamm. Evol. (1999) 6177–6213.
[21] S. Risnes, C. Li, Aspects of the final phase of enamel formation as evidenced by observations of superficial enamel of human third molars using scanning electron microscopy, Arch. Oral Biol. (2018) 8672–8679.
[22] P.M. Sander, Non-mammalian synapsid enamel and the origin of mammalian enamel prisms: the bottom-up perspective. Tooth Enamel Microstructure, CRC Press, 1997, pp. 41–62.
[23] S. Kondo, et al., The immunohistochemical localization of Bax and Bcl-2 and their relation to apoptosis during amelogenesis in developing rat molars, Arch. Oral Biol. 46 (6) (2001) 557–568.
[24] A. Balic, I. Thesleff, Tissue interactions regulating tooth development and renewal, Curr. Top. Dev. Biol. (2015) 115157–115186.
[25] J. Moradian-Oldak, Protein-mediated enamel mineralization, Front. Biosci. (Landmark. Ed) (2012) 171996–172023.
[26] J.C. Hu, et al., Proteomics and genetics of dental enamel, Cells Tissues. Organs 181 (3-4) (2005) 219–231.
[27] E. Kallenbach, The fine structure of Tomes' process of rat incisor ameloblasts and its relationship to the elaboration of enamel, Tissue Cell 5 (3) (1973) 501–524.
[28] K.S. Lester, W. von Koenigswald, Crystallite orientation discontinuities and the evolution of mammalian enamel–or, when is a prism? Scanning Microsc. 3 (2) (1989) 645–662, discussion 663.
[29] C.E.L. Smith, et al., Amelogenesis imperfecta; genes, proteins, and pathways, Front. Physiol. (2017) 8435.
[30] K. Kawasaki, K.M. Weiss, Mineralized tissue and vertebrate evolution: the secretory calcium-binding phosphoprotein gene cluster, Proc. Natl. Acad. Sci. U S. A 100 (7) (2003) 4060–4065.
[31] Y. Yamakoshi, Porcine amelogenin : alternative splicing, proteolytic processing, protein - protein interactions, and possible functions, J. Oral Biosci. 53 (3) (2011) 275–283.
[32] P.A. Fang, et al., Hierarchical self-assembly of amelogenin and the regulation of biomineralization at the nanoscale, Proc. Natl. Acad. Sci. U S A. 108 (34) (2011) 14097–14102.
[33] H.C. Margolis, E. Beniash, C.E. Fowler, Role of macromolecular assembly of enamel matrix proteins in enamel formation, J. Dent. Res. 85 (9) (2006) 775–793.
[34] C.W. Gibson, et al., Amelogenin-deficient mice display an amelogenesis imperfecta phenotype, J. Biol. Chem. 276 (34) (2001) 31871–31875.
[35] G. Gopinathan, et al., The expanded amelogenin polyproline region preferentially binds to apatite versus carbonate and promotes apatite crystal elongation, Front. Physiol. (2014) 5430.
[36] E. Beniash, J.P. Simmer, H.C. Margolis, The effect of recombinant mouse amelogenins on the formation and organization of hydroxyapatite crystals in vitro, J. Struct. Biol. 149 (2) (2005) 182–190.
[37] J. Moradian-Oldak, C. Du, G. Falini, On the formation of amelogenin microribbons, Eur. J. Oral Sci. 114 (2006). Suppl 1289-296discussion 327-289, 382.
[38] J. Moradian-Oldak, A. George, Biomineralization of enamel and dentin mediated by matrix proteins, J. Dent. Res. 100 (10) (2021) 1020–1029.
[39] H.C. Margolis, S.Y. Kwak, H. Yamazaki, Role of mineralization inhibitors in the regulation of hard tissue biomineralization: relevance to initial enamel formation and maturation, Front. Physiol. (2014) 5339.
[40] N.Y. Shin, et al., Amelogenin phosphorylation regulates tooth enamel formation by stabilizing a transient amorphous mineral precursor, J. Biol. Chem. 295 (7) (2020) 1943–1959.
[41] C.A. Stifler, et al., Loss of biological control of enamel mineralization in amelogenin-phosphorylation-deficient mice, J. Struct. Biol. 214 (2) (2022) 107844.
[42] K. Delak, et al., The tooth enamel protein, porcine amelogenin, is an intrinsically disordered protein with an extended molecular configuration in the monomeric form, Biochemistry 48 (10) (2009) 2272–2281.
[43] M.L. Paine, M.L. Snead, Protein interactions during assembly of the enamel organic extracellular matrix, J. Bone Miner. Res. 12 (2) (1997) 221–227.
[44] J.P. Simmer, M.L. Snead, Molecular biology of the amelogenin gene, in Dental Enamel: Formation to Destruction, CRC Press, Boca Raton, FL, 2017, pp. 59–84. C. Robinson, J. Kirkham, and R.C. Shore, Editors.
[45] M.L. Paine, et al., Enamel biomineralization defects result from alterations to amelogenin self-assembly, J. Struct. Biol. 132 (3) (2000) 191–200.
[46] T. Wald, et al., Intrinsically disordered proteins drive enamel formation via an evolutionarily conserved self-assembly motif, Proc. Natl. Acad. Sci. U S. A 114 (9) (2017) E1641–E1650.
[47] M.L. Paine, M.L. Snead, Tooth developmental biology: disruptions to enamel-matrix assembly and its impact on biomineralization, Orthod. Craniofac. Res. 8 (4) (2005) 239–251.
[48] J.T. Wright, et al., Relationship of phenotype and genotype in X-linked amelogenesis imperfecta, Connect. Tissue Res. 44 (2003) 172–178. Suppl.
[49] J.D. Bartlett, J.P. Simmer, New perspectives on amelotin and amelogenesis, J. Dent. Res. 94 (5) (2015) 642–644.
[50] K. Iwasaki, et al., Amelotin–a Novel Secreted, Ameloblast-specific Protein, J. Dent. Res. 84 (12) (2005) 1127–1132.
[51] A. Fouillen, et al., Interactions of AMTN, ODAM and SCPPPQ1 proteins of a specialized basal lamina that attaches epithelial cells to tooth mineral, Sci. Rep. (2017) 746683.
[52] J.Y. Sire, et al., The origin and evolution of enamel mineralization genes, Cells Tissues. Organs 186 (1) (2007) 25–48.

[53] J.E. Reseland, C.A. Heyward, A. Samara, Revisiting ameloblastin: addressing the EMT-ECM axis above and beyond oral biology, Front. Cell Dev. Biol. (2023) 11.
[54] F. Spoutil, et al., Early evolution of enamel matrix proteins is reflected by pleiotropy of physiological functions, Sci. Rep. 13 (1) (2023) 1471.
[55] M.L. Snead, Amelogenin protein exhibits a modular design: implications for form and function, Connect. Tissue Res. 44 (2003) 147–151. Suppl.
[56] S. Ali, I. Farooq, A review of the role of amelogenin protein in enamel formation and novel experimental techniques to study its function, Protein Pept. Lett. 26 (12) (2019) 880–886.
[57] S. Habelitz, Y. Bai, Mechanisms of enamel mineralization guided by amelogenin nanoribbons, J. Dent. Res. 100 (13) (2021) 1434–1443.
[58] B. Ganss, R.H. Kim, J. Sodek, Bone sialoprotein, Crit. Rev. Oral Biol. Med. 10 (1) (1999) 79–98.
[59] M.A. Icer, M. Gezmen-Karadag, The multiple functions and mechanisms of osteopontin, Clin. Biochem. (2018) 5917–5924.
[60] Y. Du, et al., Osteopontin - the stirring multifunctional regulatory factor in multisystem aging, Front. Endocrinol. (Lausanne) (2022) 131014853.
[61] A. Tacey, et al., Osteocalcin and vascular function: is there a cross-talk? Mol. Metab. (2021) 49101205.
[62] G. Karsenty, Osteocalcin: a multifaceted bone-derived hormone, Annu. Rev. Nutr. (2023) 4355–4371.
[63] J. Jia, Z. Bian, Y. Song, The role of DSPP in dentine formation and hereditary dentine defects, Chin. J. Dent. Res. 27 (1) (2024) 17–28.
[64] C. Qin, R. D'Souza, J.Q Feng, Dentin matrix protein 1 (DMP1): new and important roles for biomineralization and phosphate homeostasis, J. Dent. Res. 86 (12) (2007) 1134–1141.
[65] T. Uchida, et al., Immunochemical and immunohistochemical studies, using antisera against porcine 25 kDa amelogenin, 89 kDa enamelin and the 13-17 kDa nonamelogenins, on immature enamel of the pig and rat, Histochemistry 96 (2) (1991) 129–138.
[66] T. Uchida, et al., Immunochemical and immunocytochemical study of a 15 kDa non-amelogenin and related proteins in the porcine immature enamel: proposal of a new group of enamel proteins 'sheath proteins, Biomed. Res. 16 (3) (1995) 131–140.
[67] C.C. Hu, et al., Sheathlin: cloning, cDNA/polypeptide sequences, and immunolocalization of porcine enamel sheath proteins, J. Dent. Res. 76 (2) (1997) 648–657.
[68] R. Cerny, et al., A novel gene expressed in rat ameloblasts codes for proteins with cell binding domains, J. Bone Miner. Res. 11 (7) (1996) 883–891.
[69] P.H. Krebsbach, et al., Full-length sequence, localization, and chromosomal mapping of ameloblastin. A novel tooth-specific gene, J. Biol. Chem. 271 (8) (1996) 4431–4435.
[70] T. Wald, et al., Intrinsically disordered enamel matrix protein ameloblastin forms ribbon-like supramolecular structures via an N-terminal segment encoded by exon 5, J. Biol. Chem. 288 (31) (2013) 22333–22345.
[71] Y.H. Chun, J.C.C. Hu, J.P. Simmer, The non-amelogenins: ameloblastin and enamelin, in: M. Goldberg (Ed.), Amelogenins: Multifaceted Proteins for Dental and Bone Formation and Repair, Bentham, Sharjah, U. A. E., 2010, pp. 42–55.
[72] K. Kobayashi, et al., Splicing determines the glycosylation state of ameloblastin, J. Dent. Res. 86 (10) (2007) 962–967.
[73] Y. Yamakoshi, et al., Calcium binding of enamel proteins and their derivatives with emphasis on the calcium-binding domain of porcine sheathlin, Arch. Oral Biol. 46 (11) (2001) 1005–1014.
[74] J.D. Bartlett, J.P. Simmer, Proteinases in developing dental enamel, Crit. Rev. Oral Biol. Med. 10 (4) (1999) 425–441.
[75] X. Yang, et al., Amelogenin "nanorods" formation during proteolysis by Mmp-20, J. Struct. Biol. 176 (2) (2011) 220–228.
[76] J.P. Simmer, Kallikrein-Related Peptidase 4, in Handbook of Proteolytic Enzymes, Elsevier Academic Press, 2013, pp. 2768–2772.
[77] Y. Matsuki, et al., A compilation of partial sequences of randomly selected cDNA clones from the rat incisor, J. Dent. Res. 74 (1) (1995) 307–312.
[78] C. Robinson, et al., The developing enamel matrix: nature and function, Eur. J. Oral Sci. 106 (1998) 1282–1291. Suppl.
[79] M. MacDougall, et al., Ameloblastin gene (AMBN) maps within the critical region for autosomal dominant amelogenesis imperfecta at chromosome 4q21, Genomics 41 (1) (1997) 115–118.
[80] C.K. Mardh, et al., A nonsense mutation in the enamelin gene causes local hypoplastic autosomal dominant amelogenesis imperfecta (AIH2), Hum. Mol. Genet. 11 (9) (2002) 1069–1074.
[81] J.A. Poulter, et al., Deletion of ameloblastin exon 6 is associated with amelogenesis imperfecta, Hum. Mol. Genet. 23 (20) (2014) 5317–5324.
[82] T. Lu, et al., Whole exome sequencing identifies an AMBN missense mutation causing severe autosomal-dominant amelogenesis imperfecta and dentin disorders, Int. J. Oral Sci. 10 (3) (2018) 26.
[83] T. Liang, et al., AMBN mutations causing hypoplastic amelogenesis imperfecta and Ambn knockout-NLS-lacZ knockin mice exhibiting failed amelogenesis and Ambn tissue-specificity, Mol. Genet. Genomic. Med. 7 (9) (2019) e929.
[84] M.K. Prasad, et al., A targeted next-generation sequencing assay for the molecular diagnosis of genetic disorders with orodental involvement, J. Med. Genet. 53 (2) (2016) 98–110.
[85] F.M.F. da Silva, et al., Association between molar hypomineralization, genes involved in enamel development, and medication in early childhood: A preliminary study, Int. J. Paediatr. Dent. (2023).
[86] U. Hany, et al., Novel ameloblastin variants, contrasting amelogenesis imperfecta phenotypes, J. Dent. Res. (2023) 220345231203694.
[87] M.L. Paine, et al., A transgenic animal model resembling amelogenesis imperfecta related to ameloblastin overexpression, J. Biol. Chem. 278 (21) (2003) 19447–19452.
[88] X. Lu, et al., Ameloblastin-rich enamel matrix favors short and randomly oriented apatite crystals, Eur. J. Oral Sci. 119 (Suppl 1) (2011) 254–260. Suppl 1.
[89] J.D. Teepe, et al., Correlation of ameloblastin with enamel mineral content, Connect. Tissue Res. 55 (Suppl 1(0 1)) (2014) 38–42.
[90] P. Ma, et al., The importance of serine phosphorylation of ameloblastin on enamel formation, J. Dent. Res. 95 (12) (2016) 1408–1414.
[91] S. Fukumoto, et al., Ameloblastin is a cell adhesion molecule required for maintaining the differentiation state of ameloblasts, J. Cell Biol. 167 (5) (2004) 973–983.
[92] R.M. Wazen, et al., A mouse model expressing a truncated form of ameloblastin exhibits dental and junctional epithelium defects, Matrix. Biol. 28 (5) (2009) 292–303.
[93] Y.P. Chun, et al., Overexpression of ameloblastin in secretory ameloblasts results in demarcated, hypomineralized opacities in enamel, Front. Physiol. (2023) 141233391.
[94] T. Wald, et al., A suite of mouse reagents for studying amelogenesis, bioRxiv. (2023).
[95] F. Delsuc, B. Gasse, J.Y. Sire, Evolutionary analysis of selective constraints identifies ameloblastin (AMBN) as a potential candidate for amelogenesis imperfecta, BMC. Evol. Biol. (2015) 15148.
[96] A.G. Fincham, J. Moradian-Oldak, J.P. Simmer, The structural biology of the developing dental enamel matrix, J. Struct. Biol. 126 (3) (1999) 270–299.
[97] J. Vymetal, et al., Bioinformatic analysis and molecular modelling of human ameloblastin suggest a two-domain intrinsically unstructured calcium-binding protein, Eur. J. Oral Sci. 116 (2) (2008) 124–134.
[98] M. MacDougall, et al., Cloning, characterization and immunolocalization of human ameloblastin, Eur. J. Oral Sci. 108 (4) (2000) 303–310.
[99] P. Mazumder, et al., Amelogenin-ameloblastin spatial interaction around maturing enamel rods, J. Dent. Res. 95 (9) (2016) 1042–1048.
[100] T. Uchida, et al., Synthesis, secretion, degradation, and fate of ameloblastin during the matrix formation stage of the rat incisor as shown by immunocytochemistry and immunochemistry using region-specific antibodies, J. Histochem. Cytochem. 45 (10) (1997) 1329–1340.
[101] O. Stakkestad, et al., Phosphorylation modulates ameloblastin self-assembly and Ca (2+) binding, Front. Physiol. (2017) 8531.
[102] V. Vetyskova, et al., Characterization of AMBN I and II isoforms and study of their Ca(2+)-binding properties, Int. J. Mol. Sci. 21 (23) (2020).
[103] M. Zeichner-David, et al., Amelogenin and ameloblastin show growth-factor like activity in periodontal ligament cells, Eur. J. Oral Sci. 114 (Suppl 1244-253) (2006) discussion 254-246, 381-242.
[104] Y. Nakamura, et al., Ameloblastin fusion protein enhances pulpal healing and dentin formation in porcine teeth, Calcif. Tissue Int. 78 (5) (2006) 278–284.
[105] X. Lu, et al., The ameloblastin extracellular matrix molecule enhances bone fracture resistance and promotes rapid bone fracture healing, Matrix. Biol. (2016), 52-54113-126.
[106] J. Jacques, et al., Tracking endogenous amelogenin and ameloblastin in vivo, PLoS. One 9 (6) (2014) e99626.
[107] A.G. Fincham, et al., Evidence for amelogenin "nanospheres" as functional components of secretory-stage enamel matrix, J. Struct. Biol. 115 (1) (1995) 50–59.
[108] C. Du, et al., Supramolecular assembly of amelogenin nanospheres into birefringent microribbons, Science 307 (5714) (2005) 1450–1454.
[109] S.A. Engelberth, et al., Progression of self-assembly of amelogenin protein supramolecular structures in simulated enamel fluid, Biomacromolecules. 19 (10) (2018) 3917–3924.
[110] C. Shao, et al., Regulation of hydroxyapatite nucleation in vitro through ameloblastin-amelogenin interactions, ACS. Biomater. Sci. Eng. (2022).
[111] R.A. Bapat, J. Su, J. Moradian-Oldak, Co-immunoprecipitation reveals interactions between amelogenin and ameloblastin via their self-assembly domains, Front. Physiol. (2020) 11622086.
[112] J. Su, K.B. Chandrababu, J. Moradian-Oldak, Ameloblastin peptide encoded by exon 5 interacts with amelogenin N-terminus, Biochem. Biophys. Rep. (2016) 726–732.
[113] R.A. Bapat, J. Moradian-Oldak, Immunohistochemical co-localization of amelogenin and ameloblastin in developing enamel matrix, Methods Mol. Biol. (2019) 1922219–1922228.
[114] P. Mazumder, et al., Analysis of co-assembly and co-localization of ameloblastin and amelogenin, Front. Physiol. 5274 (2014).
[115] J. Su, et al., Ameloblastin binds to phospholipid bilayers via a helix-forming motif within the sequence encoded by exon 5, ACS. Omega 4 (2) (2019) 4405–4416.
[116] J. Su, et al., An evolutionarily conserved helix mediates ameloblastin-cell interaction, J. Dent. Res. (2020) 22034520918521.
[117] N.C. Kegulian, R. Langen, J. Moradian-Oldak, The dynamic interactions of a multitargeting domain in ameloblastin protein with amelogenin and membrane, Int. J. Mol. Sci. 24 (4) (2023).
[118] S.Y. Kwak, et al., Regulation of calcium phosphate formation by native amelogenins in vitro, Connect. Tissue Res. 55 (2014) 21–24. Suppl 1(0).
[119] S. Fukumoto, et al., Essential roles of ameloblastin in maintaining ameloblast differentiation and enamel formation, Cells Tissues. Organs 181 (3-4) (2005) 189–195.
[120] S. Hatakeyama, et al., Establishment of human dental epithelial cell lines expressing ameloblastin and enamelin by transfection of hTERT and cdk4 cDNAs, J. Oral Pathol. Med. 40 (3) (2011) 227–234.

[121] A. Kukita, et al., Primary and secondary culture of rat ameloblasts in serum-free medium, Calcif. Tissue Int. 51 (5) (1992) 393–398.
[122] P.K. DenBesten, et al., Characterization of human primary enamel organ epithelial cells in vitro, Arch. Oral Biol. 50 (8) (2005) 689–694.
[123] Q. Yan, et al., Differentiation of human ameloblast-lineage cells in vitro, Eur. J. Oral Sci. 114 (2006) 1154–1158. Suppldiscussion 164-155, 380-151.
[124] J. Chen, et al., Calcium-mediated differentiation of ameloblast lineage cells in vitro, J. Exp. Zool. B Mol. Dev. Evol. 312B (5) (2009) 458–464.
[125] A. Nakata, et al., Establishment and characterization of a spontaneously immortalized mouse ameloblast-lineage cell line, Biochem. Biophys. Res. Commun. 308 (4) (2003) 834–839.
[126] L.S. Chen, et al., Maintenance of amelogenin gene expression by transformed epithelial cells of mouse enamel organ, Arch. Oral Biol. 37 (10) (1992) 771–778.
[127] S. Kawano, et al., Establishment of dental epithelial cell line (HAT-7) and the cell differentiation dependent on Notch signaling pathway, Connect. Tissue Res. 43 (2-3) (2002) 409–412.
[128] J. Sarkar, et al., Comparison of two mouse ameloblast-like cell lines for enamel-specific gene expression, Front. Physiol. (2014) 5277.
[129] P.K. DenBesten, et al., Development and characterization of an SV40 immortalized porcine ameloblast-like cell line, Eur. J. Oral Sci. 107 (4) (1999) 276–281.
[130] A. Komine, et al., Tooth regeneration from newly established cell lines from a molar tooth germ epithelium, Biochem. Biophys. Res. Commun. 355 (3) (2007) 758–763.
[131] A. Sonoda, et al., Critical role of heparin binding domains of ameloblastin for dental epithelium cell adhesion and ameloblastoma proliferation, J. Biol. Chem. 284 (40) (2009) 27176–27184.
[132] M. Beyeler, et al., Identification of a fibronectin interaction site in the extracellular matrix protein ameloblastin, Exp. Cell Res. 316 (7) (2010) 1202–1212.
[133] H. Wang, et al., Enamel matrix protein interactions, J. Bone Miner. Res. 20 (6) (2005) 1032–1040.
[134] S. Iizuka, et al., Ameloblastin regulates osteogenic differentiation by inhibiting Src kinase via cross talk between integrin beta1 and CD63, Mol. Cell Biol. 31 (4) (2011) 783–792.
[135] Y. Zhang, et al., Ameloblastin regulates cell attachment and proliferation through RhoA and p27, Eur. J. Oral Sci. 119 (Suppl 1) (2011) 280–285. Suppl 1.
[136] X. Zhang, T.G. Diekwisch, X. Luan, Structure and function of ameloblastin as an extracellular matrix protein: adhesion, calcium binding, and CD63 interaction in human and mouse, Eur. J. Oral Sci. 119 (2011) 1270–1279. Suppl.
[137] R. Gautier, et al., HELIQUEST: a web server to screen sequences with specific alpha-helical properties, Bioinformatics. 24 (18) (2008) 2101–2102.
[138] M. Gimenez-Andres, A. Copic, B. Antonny, The many faces of amphipathic helices, Biomolecules. 8 (3) (2018).
[139] J.H. Lee, et al., Converting one-face alpha-helix mimetics into amphiphilic alpha-helix mimetics as potent inhibitors of protein-protein interactions, ACS. Comb. Sci. 18 (1) (2016) 36–42.
[140] G. van den Bergen, et al., Curved or linear? Predicting the 3-dimensional structure of alpha-helical antimicrobial peptides in an amphipathic environment, FEBS Lett. 594 (6) (2020) 1062–1080.
[141] G. Visakan, et al., Modeling ameloblast-matrix interactions using 3D cell culture, Front. Physiol. (2022) 131069519.
[142] D.G. Drubin, W.J. Nelson, Origins of cell polarity, Cell 84 (3) (1996) 335–344.
[143] W.J. Nelson, Epithelial cell polarity from the outside looking in, News Physiol. Sci. (2003) 18143–18146.
[144] R.A. Desai, et al., Cell polarity triggered by cell-cell adhesion via E-cadherin, J. Cell Sci. 122 (Pt 7) (2009) 905–911.
[145] L.N. Nejsum, W.J. Nelson, A molecular mechanism directly linking E-cadherin adhesion to initiation of epithelial cell surface polarity, J. Cell Biol. 178 (2) (2007) 323–335.
[146] F. van Roy, G. Berx, The cell-cell adhesion molecule E-cadherin, Cell Mol. Life Sci. 65 (23) (2008) 3756–3788.
[147] H. McNeill, et al., Novel function of the cell adhesion molecule uvomorulin as an inducer of cell surface polarity, Cell 62 (2) (1990) 309–316.
[148] W.J. Nelson, et al., Identification of a membrane-cytoskeletal complex containing the cell adhesion molecule uvomorulin (E-cadherin), ankyrin, and fodrin in Madin-Darby canine kidney epithelial cells, J. Cell Biol. 110 (2) (1990) 349–357.
[149] X. Guan, et al., Beta-catenin is essential for ameloblast movement during enamel development, Eur. J. Oral Sci. 124 (3) (2016) 221–227.
[150] J.D. Bartlett, et al., Targeted p120-catenin ablation disrupts dental enamel development, PLoS. One 5 (9) (2010).
[151] J.D. Bartlett, et al., MMP20 cleaves E-cadherin and influences ameloblast development, Cells Tissues. Organs 194 (2-4) (2011) 222–226.
[152] X. Guan, J.D. Bartlett, MMP20 modulates cadherin expression in ameloblasts as enamel develops, J. Dent. Res. 92 (12) (2013) 1123–1128.
[153] W.J. Nelson, D.J. Dickinson, W.I. Weis, Roles of cadherins and catenins in cell-cell adhesion and epithelial cell polarity, Prog. Mol. Biol. Transl. Sci. (2013), 1163-23.
[154] J. Chen, M. Zhang, The Par3/Par6/aPKC complex and epithelial cell polarity, Exp. Cell Res. 319 (10) (2013) 1357–1364.
[155] B. Gumbiner, Generation and maintenance of epithelial cell polarity, Curr. Opin. Cell Biol. 2 (5) (1990) 881–887.
[156] T. Inai, et al., Differential expression of the tight junction proteins, claudin-1, claudin-4, occludin, ZO-1, and PAR3, in the ameloblasts of rat upper incisors, Anat. Rec. (Hoboken) 291 (5) (2008) 577–585.
[157] K. Otsu, et al., Functional role of Rho-kinase in ameloblast differentiation, J. Cell Physiol. 226 (10) (2011) 2527–2534.
[158] G. Visakan, J. Su, J. Moradian-Oldak, Data from ameloblast cell lines cultured in 3D using various gel substrates in the presence of ameloblastin, Data Brief. (2022) 42108233.
[159] G. Visakan, J. Su, J. Moradian-Oldak, Ameloblastin promotes polarization of ameloblast cell lines in a 3-D cell culture system, Matrix. Biol. (2022) 10572–10586.
[160] J. Su, et al., Co-emergence of the amphipathic helix on ameloblastin with mammalian prismatic enamel, Mol. Biol. Evol. (2022).
[161] K.S. Lester, A. Boyde, Scanning microscopy of platypus teeth, Anat. Embryol. (Berl) 174 (1) (1986) 15–26.
[162] A.K. Mathur, P.D. Polly, The evolution of enamel microstructure: how important is amelogenin? J. Mamm. Evol. 7 (1) (2000) 23–42.
[163] A. Czogalla, et al., Attaching a spin to a protein – site-directed spin labeling in structural biology, Acta Biochim. Pol. 54 (2) (2007) 235–244.
[164] C. Li, et al., Expression and localization of amelotin, laminin gamma2 and odontogenesis-associated phosphoprotein (ODAPH) on the basal lamina and junctional epithelium, J. Mol. Histol. 53 (1) (2022) 111–118.
[165] P. Bornstein, Matricellular proteins: an overview, J. Cell Commun. Signal. 3 (3-4) (2009) 163–165.
[166] G. Nikoloudaki, Functions of matricellular proteins in dental tissues and their emerging roles in orofacial tissue development, maintenance, and disease, Int. J. Mol. Sci. 22 (12) (2021).
[167] J.E. Murphy-Ullrich, E.H. Sage, Revisiting the matricellular concept, Matrix. Biol. (2014), 371-14.
[168] J.Y. Sire, Origin and relationships of amelogenin, and the evolutionary analysis of its conserved and variable region in tetrapods, in: M. Goldberg (Ed.), Amelogenins: Multifaceted Proteins for Dental and Bone Formation and Repair, Bentham, Sharjah, U. A. E., 2010, pp. 1–18.
[169] J. Moradian-Oldak, R. Lakshminarayanan, Intrinsic disorder in amelogenin, in: M. Goldberg (Ed.), Amelogenins: Multifaceted Proteins for Dental and Bone Formation and Repair, Bentham, Sharjah, U. A. E., 2010, pp. 106–132.
[170] D. Fan, et al., In vitro study on the interaction between the 32 kDa enamelin and amelogenin, J. Struct. Biol. 166 (1) (2009) 88–94.
[171] D. Fan, et al., The cooperation of enamelin and amelogenin in controlling octacalcium phosphate crystal morphology, Cells Tissues. Organs 194 (2-4) (2011) 194–198.
[172] Y. Zou, et al., Determination of protein regions responsible for interactions of amelogenin with CD63 and LAMP1, Biochem. J. 408 (3) (2007) 347–354.
[173] H. Zhang, et al., Full length amelogenin binds to cell surface LAMP-1 on tooth root/periodontium associated cells, Arch. Oral Biol. 55 (6) (2010) 417–425.
[174] C. Connelly, et al., Dynamic interactions of amelogenin with hydroxyapatite surfaces are dependent on protein phosphorylation and solution pH, Colloids. Surf. B Biointerfaces. (2016) 148377–148384.
[175] S.B. Lokappa, et al., Interactions of amelogenin with phospholipids, Biopolymers 103 (2) (2015) 96–108.
[176] S.B. Lokappa, K.B. Chandrababu, J. Moradian-Oldak, Tooth enamel protein amelogenin binds to ameloblast cell membrane-mimicking vesicles via its N-terminus, Biochem. Biophys. Res. Commun. 464 (3) (2015) 956–961.
[177] J.T. Wright, Consequences of amelogenin mutations: implications in amelogenesis imperfecta, in: M. Goldberg (Ed.), Amelogenins: Multifaceted Proteins for Dental and Bone Formation and Repair, Bentham, Sharjah, U. A. E, 2010, pp. 88–98.